Geologica Acta, Vol.16, Nº 1, March 2018, 45-64
DOI: 10.1344/GeologicaActa2018.16.1.3

geologica acta

Organic petrology and geochemistry of mudstones from the lower Shahejie Formation in the Tanggu area of eastern China: evidence for the presence of an ancient saline lake

L. LI[1,2] G.Q. YAO[2] M.J. CAI[3] Y.H. LIU[3]

[1]Research Institute of Exploration and Development, Sinopec Jianghan Oilfield Companye
Wuhan, PR China. E-mail: santali2005@gmail.com; Tel: +86-13387620885

[2]Key Laboratory of Tectonics & Petroleum Resources of the Ministry of Education of China, University of Geosciences
Wuhan 430074, PR China

[3]PetroChina Dagang Oilfield Company
Tianjin 300280, PR China

ABSTRACT

Mudstones in the Sha-3 member of the Shahejie Formation, in the Tanggu area of the Huanghua Depression, have been found to contain analcime and ankerite. Hydrothermal sedimentation has been invoked to explain the origin of these two minerals, raising the question of whether hydrothermal activity occurred at a sufficient scale to significantly raise the salinity of the depositional environment. We applied a suite of organic petrological and geochemical methods to directly address this question. Maceral composition, kerogen type, and the distribution of *n*-alkanes, hopanes, and steranes indicate that the organic matter contained in these mudstones and dolomitic mudstones is mainly derived from algae and bacteria. The dominant acritarch genera, $C_{31}R/C_{30}$ hopane ratio, gammacerane index, Pr/Ph ratio, and the relationship between Pr/*n*-C_{17} and Ph/*n*-C_{18} suggest that the mudstones and dolomitic mudstones were deposited in an anoxic, saline lacustrine environment. T_{max}, biomarker maturity indices, the Thermal Alteration Index (TAI) and Acritarch Alteration Index (AAI), and vitrinite reflectance all indicate that the organic matter is at an immature to early mature stage. The estimated maximum paleotemperature is close to the present-day burial temperature, and much lower than the homogenization temperature of the analcime veins in dolostones. Combined with the absence of unresolved complex mixtures on the *n*-alkane pattern, this suggests that hydrothermal activity had a negligible impact on the salinity and alkalinity of the depositional lake.

KEYWORDS | ***n*-alkanes. Burial temperature. Organic matter. Salinity. Hydrothermal activity. Stratification.**

INTRODUCTION

Analcime- and carbonate- bearing mudstones have long been interpreted as the product of a saline environment (Gall and Hyde, 1989; Remy and Ferrell, 1989; Ingles *et al*., 1998; Do Campo *et al*., 2007). The presence of such deposits in the lower Shahejie Formation (Fm.) (Sha-3-5 submember) of the Tanggu area, eastern China (Fig. 1A), suggests that these sediments were deposited in an ancient saline lake. However, the underlying analcime-bearing dolostones (Qu *et al*., 2014; Li *et al*., 2015a) and the hydrothermal sedimentation hypothesis (Zheng *et al*., 2006) provide a new perspective to re-examine the picture. Introduced by Zheng *et al*. (2006) to explain the origin of laminated analcime-bearing dolostones in lacustrine environments, this hypothesis quickly won the approval of numerous Chinese researchers (Liu *et al*., 2012; Song *et al*., 2015;

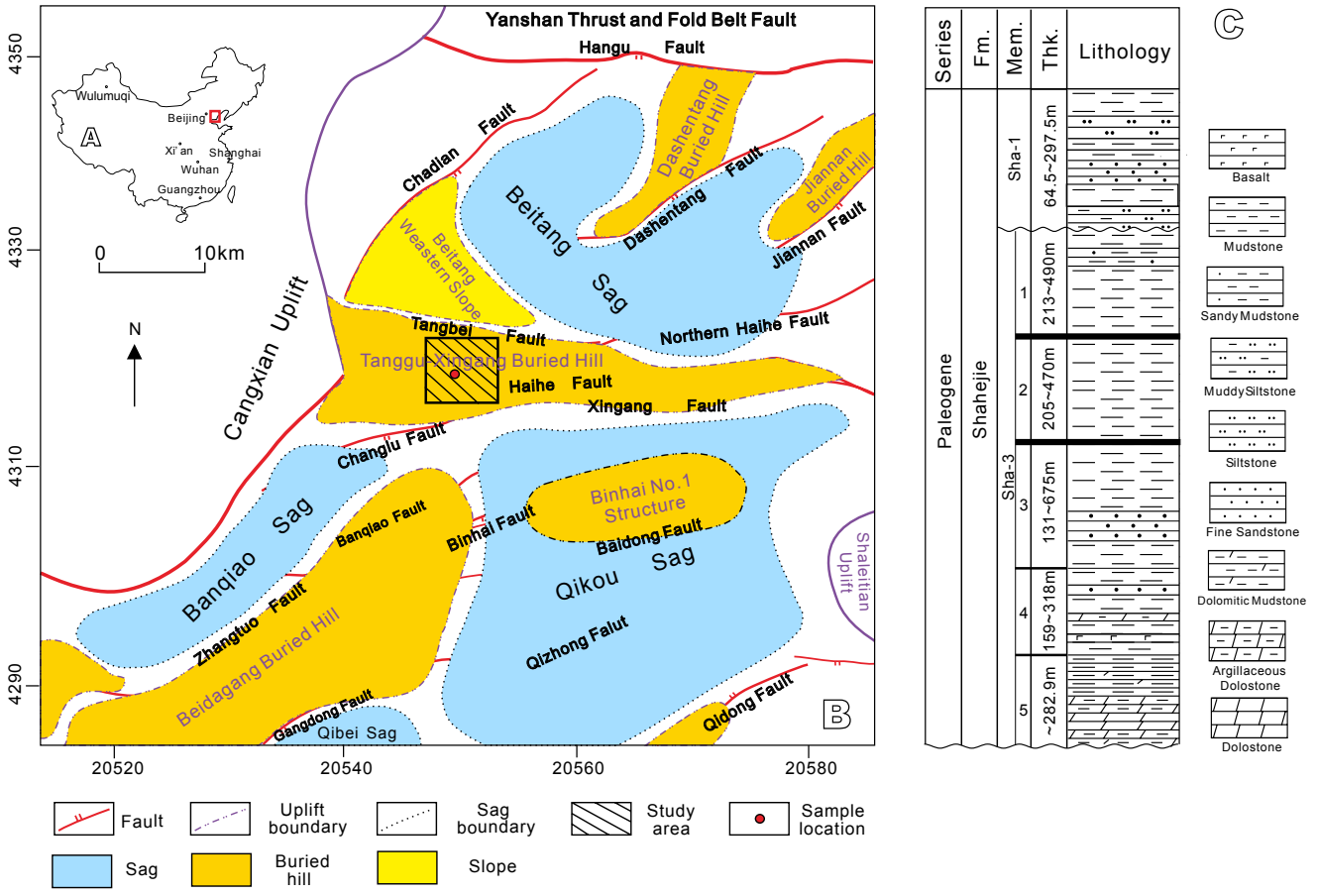

FIGURE 1. A) Location map; B) Geological map of the Tanggu area in the Huanghua depression; C) Generalized stratigraphic section of the Paleogene Shahejie in the study area, modified from Zhou *et al.*, 2011.

Zhong *et al.*, 2015). However, some other researchers voiced doubts about hydrothermal sedimentation, due to the uncertainty of the sediment source and scant evidence for high-temperature alteration (Li and Yao, 2016).

Ion-rich hydrothermal fluids do potentially have the ability to imprint freshwater sediments with some characteristic features of saline environments, a process that can be observed in the Lake Tanganyika (Tiercelin *et al.*, 1993) and Yellowstone (Morgan, 2007), where hydrothermal systems are well developed. Previous studies did not report analcime or ankerite in the mudstones of the Sha-3 Member in the Huanghua Depression. Furthermore, the dark mudstones of the Sha-3 Member at the entire Bohaiwan Basin have been interpreted to have been deposited in fresh to brackish water (Chen *et al.*, 1994; Yao *et al.*, 1994; Ryder *et al.*, 2012). Therefore, while the hydrothermal sedimentation hypothesis lacks definitive proof, it remains a potential explanation for certain unusual features of the mudstones overlying analcime-bearing dolostone succession.

Organisms are sensitive to changes in salinity (Cohen, 2003), and organic matter is subject to varying degrees of thermal alteration (Farrimond *et al.*, 1998). These features can potentially help to reveal the nature of the depositional environment, and evaluate the influence (if any) of hydrothermal activity. This study aims to use organic petrological and geochemical data to: i) determine the origin of organic matter and reconstruct the depositional environment; ii) determine whether hydrothermal activity played a role in the formation of the saline lake.

GEOLOGIC SETTING

The Tanggu area, in the northwestern Huanghua Depression, sits atop the Tanggu-Xingang buried hill structure. The Tangbei and Haihe faults separate the Tanggu area from the surrounding structural elements, namely the Beitang western slope, the Beitang sag, the Qikou sag, and the Banqiao sag (Fig. 1B).

The Shahejie Fm. is an Eocene-Oligocene sedimentary unit, deposited during a period of subsidence related to multiple stages of rifting in the Tanggu area (Zhang *et al.*, 2009). Three members can be distinguished in the Shahejie Fm., denoted (in ascending order) as the Sha-3, Sha-2, and Sha-1 members. The Sha-3 and Sha-2 members were deposited during the first period of rifting, and the Sha-1 Member corresponds to the second rifting interval (Huang *et al.*, 2008). The Sha-2 Member in the Tanggu area experienced severe erosion during a period of uplift, leading to an unconformable contact between the Sha-3 and Sha-1 members (Fig. 1C). Based on detrital mineral assemblages and the direction of sediment transport, Huang *et al.* (2009) proposed that the sediments of the Sha-3 Member were sourced mainly from the Yanshan fold-and-thrust belt and the Cangxian uplift. Furthermore, Li *et al.* (2015b) argued that the sediments of the lower part of the Sha-3 Member were derived primarily from felsic rocks in the Yanshan fold-and-thrust belt, based on their element geochemistry.

The Sha-3 Member is the most important lacustrine petroleum source rock in the Huanghua Depression (a unit of the Bohaiwan Basin) (ECPG-Dagang, 1991; Ryder *et al.*, 2012). Several facies associations reflect lacustrine and nearshore environments (Cheng-Yong, 1991; Allen *et al.*, 1997). Some researchers proposed that the deposition of the Sha-3 Member occurred during a marine transgression in the light of the presence of special minerals (glauconite and apatite), dinoflagellates, acritarchs, trace fossils (He and Yu, 1982; Yao *et al.*, 1992; Yuan *et al.*, 2005, 2006). However, well-established evidence is still lacking and the topic remains controversial (Yao *et al.*, 1992; Sun *et al.*, 1996). In the Tanggu area, the Sha-3 Member is divided into 5 submembers based on sedimentary cycles (Sha-3-5 to Sha-3-1, in ascending order) (Fig. 1C). Fan-deltas, gravity-slides, and lake deposits occur alternatively in vertical direction during the different stages of deposition under the control of the tectonic framework and source areas (Deng *et al.*, 2006; Huang *et al.*, 2009). The Sha-3-5 submember comprises 282.9m of semi-deep water lacustrine deposits, consisting primarily of light-gray laminated or massive dolostones, gray argillaceous dolostones with laminated and massive structures; and deep water lacustrine deposits principally of brown-gray to dark-gray laminated dolomitic mudstones, and black mudstones. The Sha-3-4 (159-318m) and Sha-3-3 (131-675m) submembers consist of fan delta and gravity-slide deposits, composed of a total of 290 to 993m of dark-gray mudstones and fine sandstones; basaltic layers occur occasionally in the Sha-3-4 submember. The Sha-3-2 submember is composed of 205 to 470m, and the Sha-3-1 of 213 to 490m, therefore, both submembers altogether are composed of 418 to 960m of dark-gray mudstones, grading into sandy mudstones toward the top of the succession. The Sha-1 Member, which has not been studied in detail, consists of 64.5 to 297.5m of pale gray to dark-gray mudstones and muddy siltstones, interbedded with gray siltstones to fine sandstones.

The dolostones and argillaceous dolostones of the Sha-3-5 submember are completely wraped within the mudstones and dolomitic mudstones, forming an ellipsoidal geobody with a three-layer-structure. The inner layer is formed by dolostones, the middle layer consists mostly of argillaceous dolostones and dolomitic mudstones, and the outer layer is composed of mudstones (Fig. 2A). Those dolomitic facies (dolostones and argillaceous dolostones), which were interpreted as the product of seepage-reflux dolomitization (Wang *et al.*, 2014), contain ankerite, analcime, quartz, albite, orthoclase, and illite; the presence of vugs in the massive dolostones may suggest other evaporites had developed (and been dissolved afterwards) as the original brine concentrated (Li *et al.*, 2015b). Analcime in the dolomitic facies has two modes of occurrence: i) aphanocrystalline analcime-rich lamina; ii) finely-finely crystalline analcimes fillings of veinlets and vugs. Ankerite can also occur as ankerite-rich lamina, but the development of this type of lamina is largely attributed to the mixing of other limited minerals (Li *et al.*, 2015b). The overlying mudstones (Fig. 2B; C) have similar mineral assemblages, textures, and occurrences to dolomitic facies, but contain fewer microfractures and more clay minerals (Fig. 2D; E).

SAMPLING AND METHODS

A total of 35 fresh rock samples were collected from the core of well T12C, in the Tanggu area. This set included 24 samples of laminated mudstone, and 11 samples of laminated dolomitic mudstone.

Polished thin sections and strew-mounted slides of 8 samples were prepared for organic petrological analysis. Maceral composition was determined under transmitted, reflected, and fluorescent light using a Leica fluorescence microscope. Vitrinite reflectance was measured using a Leica MSP200 microspectrophotometer.

All 35 samples were crushed to a powder, and 100mg of each powdered sample was prepared for Rock-Eval (Espitalié *et al.*, 1985) pyrolysis using an OGE II oil and gas evaluation workstation. Chinese National Standard GB/T 18602-2001 was used to assess data quality.

We obtained extracts from 4 powdered samples, using a YS_B-automatic multifunction extractor with chloroform as

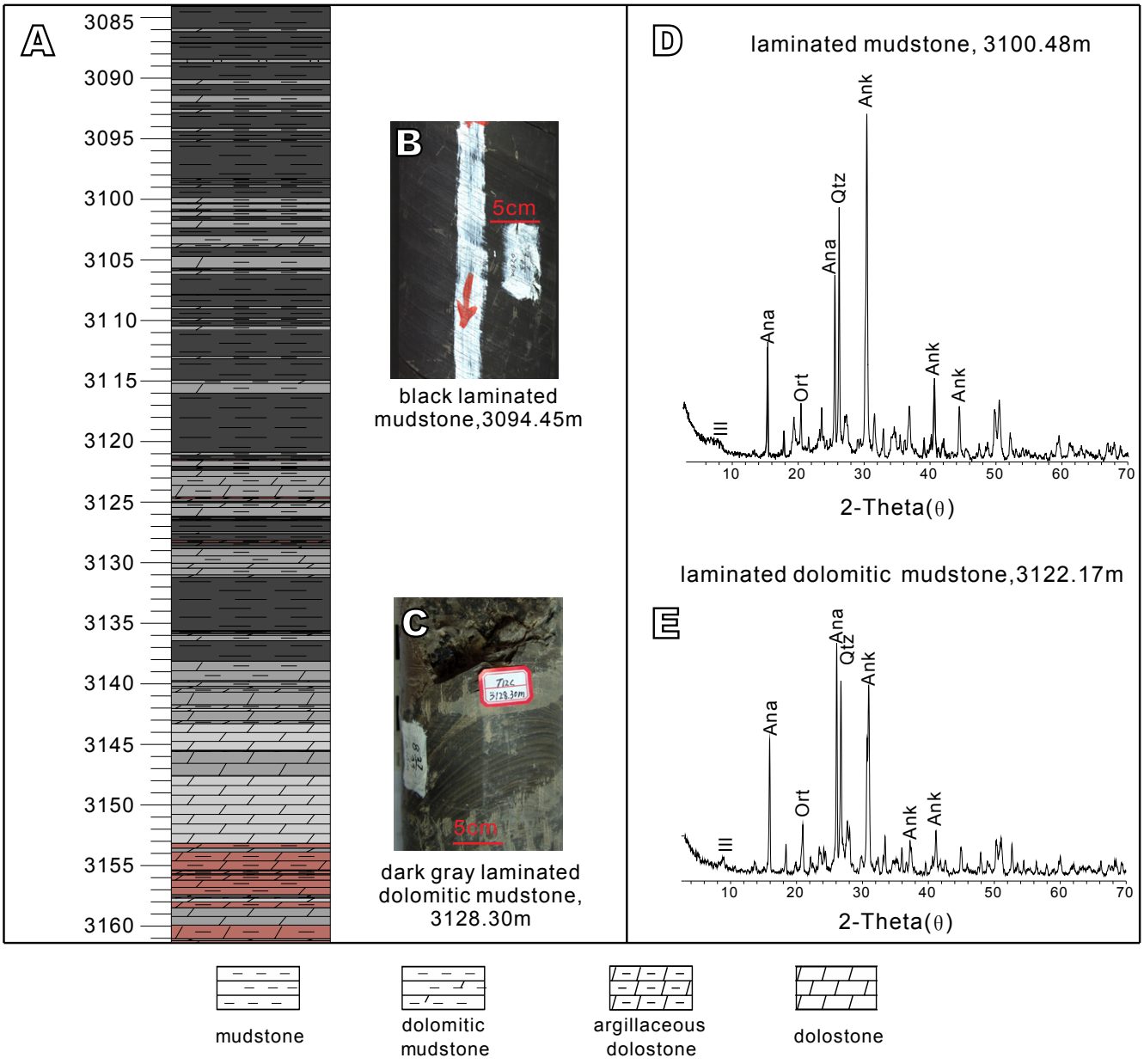

FIGURE 2. A) Lithological section of the Sha-3-5 submember in borehole T12C in the Tanggu area. B) Representaive laminated mudstone; C) Representaive laminated dolomitic mudstone; D) Representative XRD pattern of laminated mudstone; E) Representative XRD pattern of laminated dolomitic mudstone.

the eluent. Saturated hydrocarbon, aromatic hydrocarbon, and NSO compound fractions were sequentially separated from the extracts, using a silica gel-alumina column with *n*-hexane, dichloromethane, pure ethyl alcohol, and chloroform as eluents.

The aliphatic fraction was prepared for Gas Chromatography (GC) and Gas Chromatography-Mass Spectrometry (GC-MS). GC analyses were performed on an Agilent 7890A gas chromatograph. The GC oven temperature was increased from 80°C to 310°C at a rate of 5°C/min, then held isothermally at 310°C for 20 min. Nitrogen was used as carrier gas. GC-MS analyses were made on an Agilent 6890N gas chromatograph, coupled to an Agilent 5973N mass spectrometer. The GC-MS oven temperature was programmed to increase from 80°C to 300°C at a rate of 4°C/min, then hold isothermally at 300°C for 20 min. Helium was used as a carrier gas.

Chinese Professional Standards SY/T 5118-2005 and SY/T 5119-2008 and Chinese National Standard GB/T 18606-2001 were used to assess data quality.

Analyses were performed mainly at the Petroleum Geologic Test Center of the Petroleum Exploration and Development Research Institute, Jianghan Oilfield Company, SINOPEC.

RESULTS

Organic petrography

Liptinite is the predominant maceral group in the mudstones of the Sha-3-5 submember, with lamalginite and telalginite being the two most common macerals. Lamalginite occurs in both laminated mudstones and laminated dolomitic mudstones, while telalginite is present only in laminated dolomitic mudstones.

Lamalginite has two distinct modes of occurrence, in organic matter-rich laminae, appearing as thin yellow lineaments under ultraviolet light (Fig. 3A), and secondarily as randomly dispersed organic matter (Fig. 3B; C). Telalginite is typically distributed evenly in a more or less horizontal line, ranging from 20 to 150μm in diameter. The amorphous organic matter, frequently observed in strew-mounted slides, it is likely to associate with lamalginite and telalginite (Fig. 4A; B). Sporopolleninite (Figs. 3C and 4A; C), chlorophyllinite (Fig. 3A), and subrinite (Fig. 4D) are also present in laminated mudstone, but in small amounts. Inertinite is the least common maceral group, with inertoderinite generally predominating over funsinite (Fig. 3B; C). Vitrinite is scarce to absent in most of the rock samples.

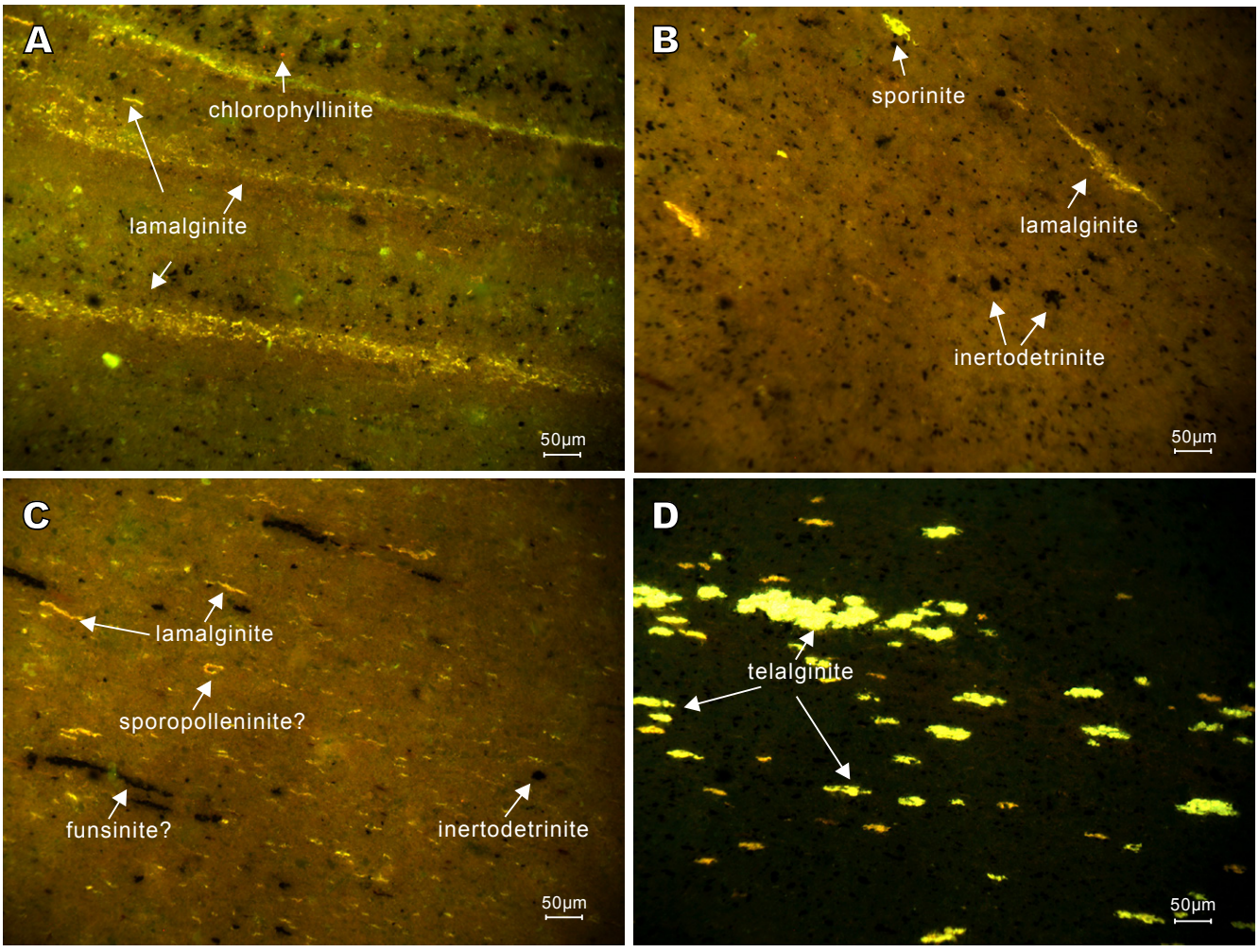

FIGURE 3. Ultraviolet light microphotographs of organic matter in the Sha-3-5 submember of the Tanggu area: A) lamalginite accumulated as organic matter-rich lamina and randomly dispersed, and cholorophyllinite in laminated mudstone; B) lamalginite, sporopolleninite and inertodetrinite sporadically dispersed in laminated mudstone; C) lamalginite and sporopolleninite(?), funsinite(?) and inertodetrinite dissiminated in laminated mudstone; D) telalginite scattered in laminated dolomitic mudstone.

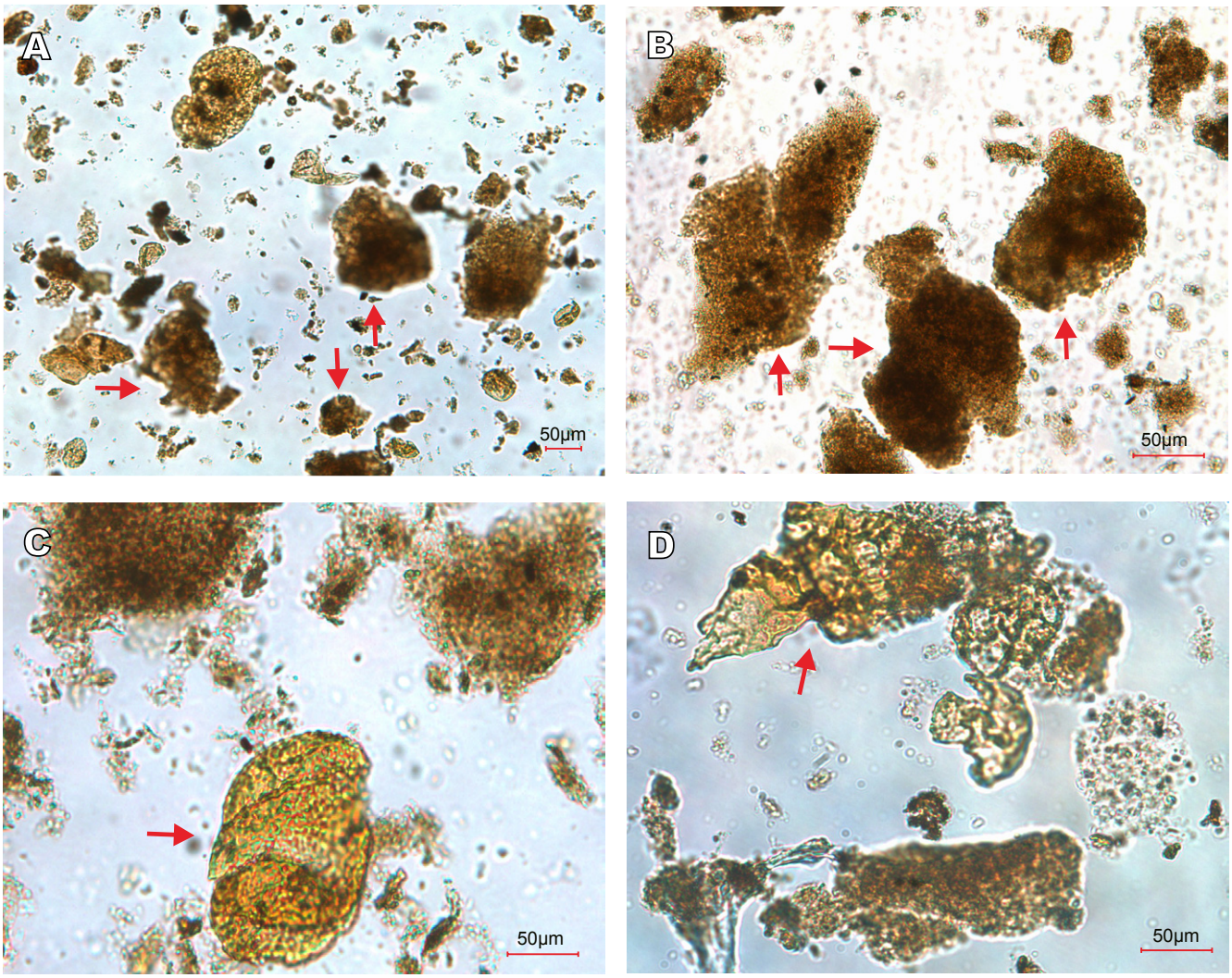

FIGURE 4. Amorphous organic matter in the Sha-3-5 submember of the Tanggu area: A) amorphous organic matter, some sporopolleninite can also be observed in laminated mudstone; B) amorphous organic matter in laminated dolomitic mudstone; C) sporinite in laminated mudstone; D) suberinite in laminated mudstone.

Acritarchs and algae occur in all samples, being acritarchs especially abundant. *Dictyotidium*, *Granodisus*, and *Rugasphacra* are the principal acritarch genera, and *Hungarodiscus*, *Membranilarnacia*, and *Paraperidinium* are the predominant algal genera (Fig. 5).

Only three pieces of vitrinite could be discerned in two samples, yielding values of 0.65% and 0.78% (Table 1).

Total Organic Carbon and Rock-Eval pyrolysis

Total Organic Carbon (TOC) ranges from 0.75 to 3.36wt.% in laminated mudstones, and from 0.95 to 2.85wt.% in laminated dolomitic mudstones (Table 2). T_{max} values range from 424 to 440°C in laminated mudstones, and from 437 to 444°C in laminated dolomitic mudstones. Laminated mudstones show Rock-Eval S_1 values ranging from 0.45 to 3.86mg HC/g, while the laminated dolomitic mudstones show slightly lower values, ranging from 0.25 to 2.73mg HC/g. Hydrogen Index (HI) values vary from 318 to 670mg HC/g in laminated mudstones, and from 293 to 655mg HC/g in laminated dolomitic mudstones. In general, mudstone samples show higher TOC, S_1 and HI values than dolomitic mudstones, suggesting that lithology played a role in the accumulation of organic matter.

Molecular composition of organic matter

n-alkanes and Isoprenoids

All samples show a similar *n*-alkane distribution. The carbon number of *n*-alkanes ranges from *n*-C_{12} to *n*-C_{36}, with local maxima at *n*-C_{15}, *n*-C_{17}, *n*-C_{23}, and *n*-C_{31}.

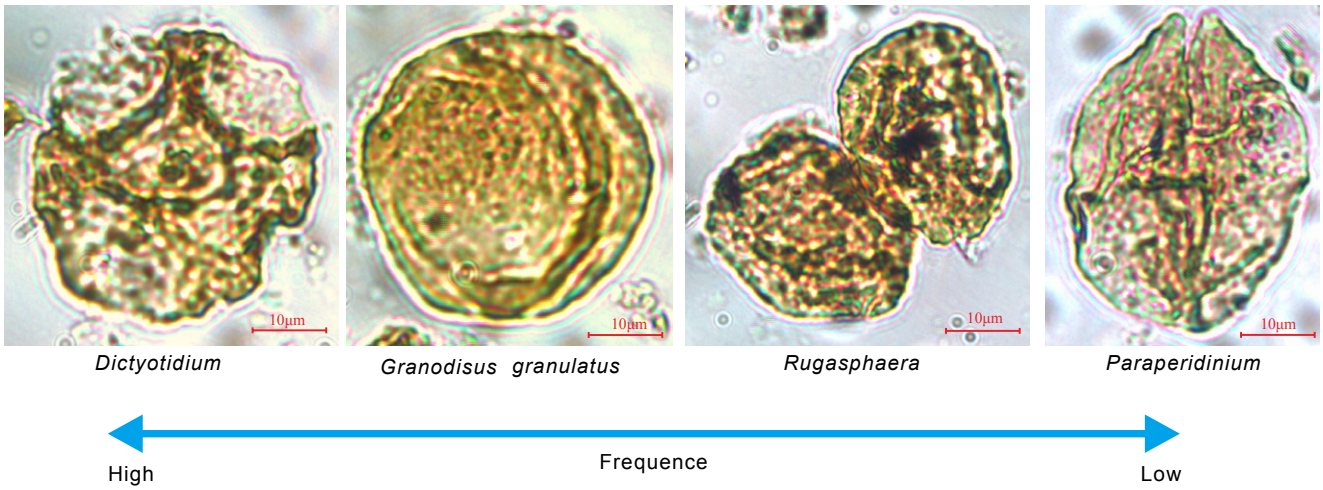

FIGURE 5. Acritarchs and algae from the Sha-3-5 submember of the Tanggu area. A) *Dictyotidium* in laminated mudstone; B) *Granodisus granulatus* in laminated dolomitic mudstone; C) *Rugasphaera* in laminated dolomitic mudstone; D) *Paraperidinium* in laminated mudsonte.

Short-chain (n-C_{12}-n-C_{20}) and mid-chain (n-C_{21}-n-C_{25}) n-alkanes are more abundant than long-chain (n-C_{26}-n-C_{36}) n-alkanes (Fig. 6). The CPI (Carbon Preference Index, $=((C_{25}+C_{27}+C_{29}+C_{31}+C_{33})/(C_{24}+C_{26}+C_{28}+C_{30}+C_{32})+(C_{25}+C_{27}+C_{29}+C_{31}+C_{33})/(C_{26}+C_{28}+C_{30}+C_{32}+C_{34}))/2)$, proposed by Bray and Evans (1961), ranges from 1.00 to 1.28, showing no clear odd-even predominance for sample O1 and odd predominance for samples O15, O31, and O39 (Table 3).

Acyclic isoprenoids occur at considerable abundances in all samples. Phytane (Ph) is evidently abundant over the n-alkanes and pristane (Pr), while pristane is less abundant than n-C_{17}. The Pr/n-C_{17} and Ph/n-C_{18} values range from 0.59 to 0.96 and 3.49 to 7.13 respectively (Table 3).

Terpanes

All samples contained abundant pentacyclic terpanes (hopanes), and some component of tricyclic terpanes. Identified pentacyclic terpanes, in order of decreasing abundance, include C_{30} hopane, gammacerane, C_{29} norhopane, C_{31} diahopane, C_{30} moretane, C_{30} oleanane, 17a (H)-trisnorhopane (T_m), homohopanes (C_{31}–C_{35}), and 18a (H)-trisnorhopane (T_s) (Fig. 7).

The abundance of C_{29} norhopane is much lower than that of C_{30} hopane, with the C_{29}/C_{30} hopane ratio ranging from 0.20 to 0.38. T_m dominates over T_s (Table 3). The homohopane distribution exhibits a decreasing trend, from high-number homohopanes towards low-number homohopanes. Oleanane/hopane values range from 0.01 to 0.1.

TABLE 1. Vitrinite reflectance of laminated mudstones and laminated dolomitic mudstones from the Sha-3-5 submember of the Tanggu area

Sample No.	Depth(m)	Lithology	R_0(%)	Measuring points	Standard deviation
O1	3084.09	LM	/	/	/
O11	3094.80	LM	/	/	/
O15	3099.23	LM	0.78	2	0.2051
O23	3107.58	LM	/	/	/
O31	3115.99	LM	/	/	/
O35	3121.20	LM	/	/	/
O39	3129.47	LDM	/	/	/
O40	3132.30	LM	0.65	1	0.0000

Note: LM=Laminated Mudstone; LDM=Laminated Dolomitic Mudstone;
/ = not determined; similarly hereinafter

TABLE 2. Rock-Eval pyrolysis data of laminated mudstones and laminated dolomitic mudstones from the Sha-3-5 submember of the Tanggu area

Sample No.	Depth	Lithology	T_{max} (℃)	TOC (wt.%)	S_1 (mg HC/g rock)	S_2 (mg HC/g rock)	S_1+S_2 (mg HC/g rock)	HI (mg HC/g TOC)	Kerogen type
O1	3084.09	LM	424	0.75	0.45	2.39	2.84	318.67	II-III
O2	3085.16	LM	431	2.21	1.70	12.59	14.29	569.68	II
O7	3090.37	LDM	443	1.21	0.25	3.55	3.80	293.39	II-III
O11	3094.80	LM	436	1.42	0.63	6.09	6.72	428.87	II
O12	3095.40	LM	432	2.02	1.14	9.79	10.93	484.65	II
O13	3096.30	LM	437	2.36	1.38	13.00	14.38	550.85	II
O14	3097.48	LM	436	3.07	1.97	17.17	19.14	559.28	II
O15	3099.23	LM	439	2.24	1.18	11.98	13.16	534.82	II
O16	3099.90	LM	439	2.30	1.09	13.11	14.20	570.00	I
O17	3100.28	LM	438	2.17	0.99	10.51	11.50	484.33	II
O18	3100.78	LDM	444	1.69	0.39	7.68	8.07	454.44	II
O19	3102.41	LM	440	2.22	1.30	12.08	13.38	544.14	II
O20	3103.34	LDM	444	1.91	1.41	11.74	13.15	614.66	I
O21	3105.14	LDM	443	2.40	1.62	14.46	16.08	602.50	I
O22	3106.84	LM	444	2.74	1.07	15.54	16.61	567.15	II
O23	3107.58	LM	440	2.18	0.84	11.63	12.47	533.49	II
O24	3108.53	LM	442	1.90	0.71	8.68	9.39	456.84	II
O25	3109.50	LM	441	2.65	0.96	15.73	16.69	593.58	I
O26	3110.39	LM	437	2.69	1.17	14.95	16.12	555.76	II
O27	3111.20	LM	444	3.36	1.58	21.66	23.24	644.64	I
O28	3113.00	LDM	441	2.85	2.10	18.67	20.77	655.09	I

Geologica Acta, 16(1), 45-64 (2018)
DOI: 10.1344/GeologicaActa2018.16.1.3

TABLE 2. (Cont.)

Sample No.	Depth	Lithology	T_{max} (℃)	TOC (wt.%)	S_1 (mg HC/g rock)	S_2 (mg HC/g rock)	S_1+S_2 (mg HC/g rock)	HI (mg HC/g TOC)	Kerogen type
O29	3113.79	LM	441	3.24	2.05	21.65	23.70	668.21	I
O30	3115.01	LDM	441	2.25	2.14	14.10	16.24	626.67	I
O31	3115.99	LM	442	2.49	1.87	15.87	17.74	637.35	I
O32	3116.50	LM	443	1.00	0.66	4.23	4.89	423.00	II
O33	3119.44	LM	440	1.54	0.88	7.47	8.35	485.06	II
O34	3121.00	LDM	441	0.95	0.79	4.25	5.04	447.37	II
O35	3121.20	LM	442	1.67	1.12	10.34	11.46	619.16	I
O36	3122.52	LDM	440	1.77	1.32	10.63	11.95	600.56	I
O37	3123.60	LDM	437	1.29	1.02	7.50	8.52	581.40	II
O38	3127.50	LDM	442	2.74	2.73	17.33	20.06	632.48	I
O39	3129.47	LDM	441	1.95	1.03	11.31	12.34	580.00	II
O40	3132.30	LM	442	2.70	2.47	17.49	19.96	647.78	I
O41	3135.67	LM	439	2.80	3.86	15.44	19.30	551.43	II
O42	3137.89	LM	443	2.40	2.15	16.10	18.25	670.83	I

TABLE 3. Summary of *n*-alkane and isoprenoids and biomarker ratios calculated from m/z 217 and m/z 191 mass fragmentograms of laminated mudstones and laminated dolomitic mudstones extract from the Sha-3-5 submember of the Tanggu area

Sample No.	*n*-alkane and isoprenoids				Terpanes						Steranes				
	Pr/Ph	Pr/*n*-C_{17}	Ph/*n*-C_{18}	CPI	C_{29}/C_{30}	T_s/T_m	C_{31} 22S(22S+22R)	Moretanes /hopanes	Oleanane index	Gammacerane index	C_{29} 20S/(20R+20S)	C_{29} ββ/(αα+ββ)	Regular steranes(%)		
													C_{27}	C_{28}	C_{29}
O1	0.22	0.96	5.73	1.00	0.38	0.18	0.60	0.18	0.10	3.31	0.25	0.24	34.81	27.47	37.31
O15	0.36	0.81	7.13	1.11	0.21	0.23	0.59	0.16	0.03	2.30	0.20	0.21	29.80	31.06	38.66
O31	0.34	0.59	4.44	1.14	0.20	0.22	0.55	0.17	0.02	2.08	0.22	0.21	20.32	33.55	45.75
O39	0.37	0.68	3.49	1.28	0.24	0.20	0.52	0.23	0.01	2.70	0.20	0.21	22.60	31.44	45.47

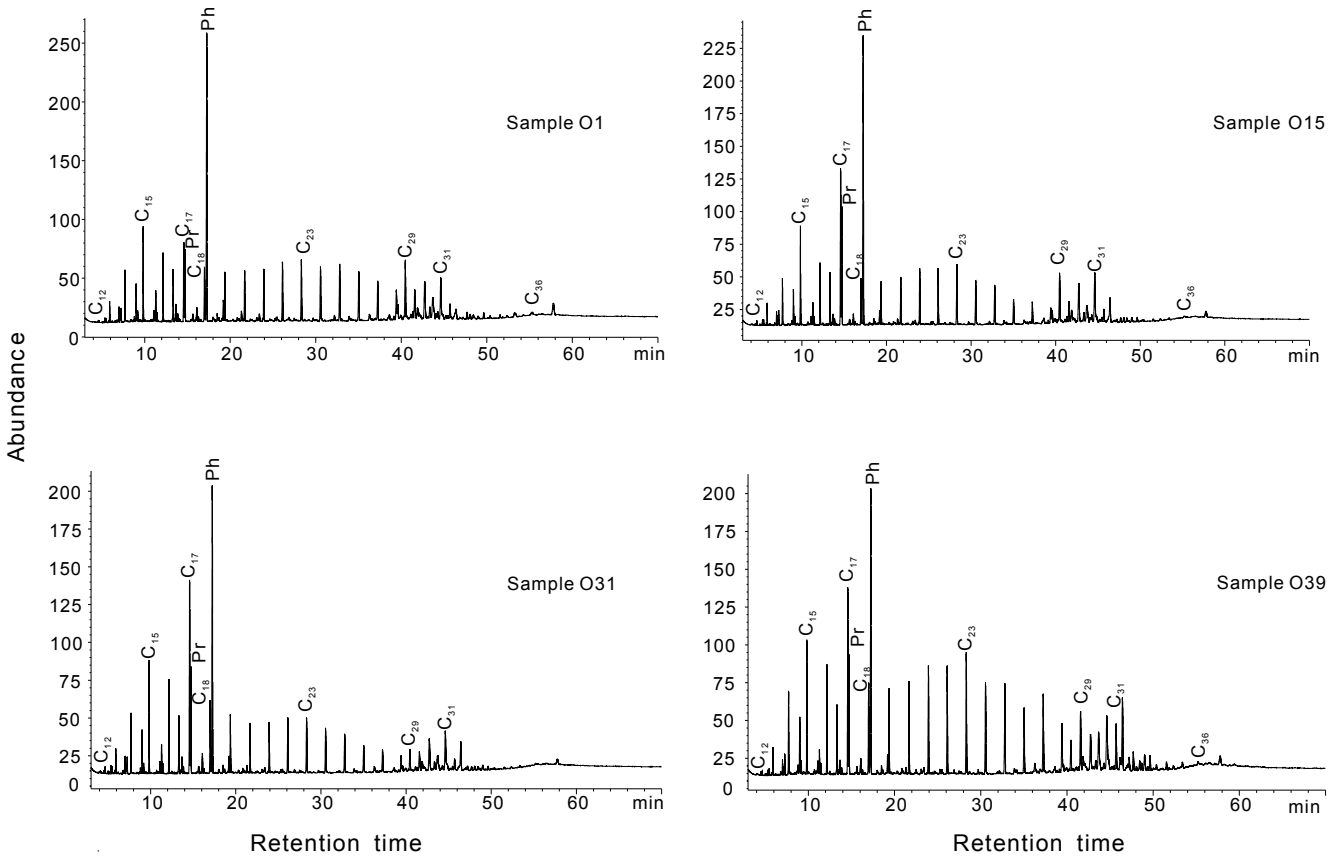

FIGURE 6. Gas Chromatograms (GC) of saturated hydrocarbons of laminated mudstones and laminated dolomitic mudstones from the Sha-3-5 submember of the Tanggu area.

Tricyclic terpanes identified in our samples range from C_{19} to C_{26}, with C_{20}, C_{21}, and C_{23} being the most abundant (Fig. 7).

Steranes

Regular steranes were the most abundant sterane type, though small amounts of diasteranes, pregnane, and homopregnane were identified in all samples (Fig. 8).

The regular sterane distribution can be characterized as C_{27}>C_{29}>C_{28} in samples O1 and O15, C_{29}>C_{28}>C_{27} in sample O31, and C_{29}>C_{27}>C_{28} in sample O39. The C_{29}20S/(20R+20S) ratio ranges from 0.20 to 0.25, while the $C_{29}\beta\beta/(\alpha\alpha+\beta\beta)$ ratio ranges from 0.21 to 0.24 (Table 3).

DISCUSSION

Origin of organic matter and depositional environment

Organic petrology reveals that lamalginite and telalginite are the dominant forms of organic matter in our samples. The telalginite is always related to algae, while the lamalginite can derive from either microbial mat or algae (Tyson, 1995). Organic matter-rich laminae, related to lamalginite are widely reported in lacustrine oil shales and mudstones, for example in the oil shales of the Green River Fm. in Wyoming and Utah (Schieber *et al.*, 2007) and the Messinian Fm. in the Lorca Basin (Permanyer *et al.*, 1994), and in the dolomitic mudstones of the Lucaogou Fm. in the Jiuxi Basin (Tu *et al.*, 2012) and the Fengcheng Fm. in the Junggar Basin (Jian *et al.*, 2015). Schieber *et al.* (2007) proposed that the organic laminae with considerable lateral persistence in the Green River Fm. would have had a benthic microbial origin rather than a plankton-derived origin. The high similarity between their and our case inclined us apply this interpretation to our samples. Amorphous Organic Matter (AOM) is also abundant in our rock samples and this type of organic matter may derive from bacteria or algae (Largeau *et al.*, 1990; Permanyer *et al.*, 2016). Pacton *et al.* (2011) proposed that microbes take part in the AOM formation by microbial reworking of terrestrial fragments and primary microbial populations. Thus, a significant contribution of bacteria to the organic matter can also be deduced from the abundant AOM. Vascular plant input was minimal as little inertinite and vitrinite component was observed in our samples.

Organic geochemical characteristics of laminated mudstones and laminated dolomitic mudstones are consistent with our inferences from organic petrology. The correlation between T_{max} and HI reveals a predominance of Type I and Type II kerogen (Fig. 9), suggesting that most of the organic matter was derived from algae, mixed plankton, and bacterial debris (Peters *et al.*, 2005b). This is further supported by the biomarker characteristics of the organic material.

The predominance of short- and mid-length *n*-alkanes suggests that the dominant sources of organic matter were benthic bacteria, phytoplankton, and zooplankton (Brassell *et al.*, 1978; Adegoke *et al.*, 2014; Yang *et al.*, 2015). The dominance of phytane over pristane and *n*-alkane is not ubiquitous in fine-grained sedimentary rocks (shales or mudstones). One comparable case is the saturated hydrocarbon of the Laney Shale of the Washakie Basin but no further origin and interpretation of such phenomenon was given (Horsfield *et al.*, 1994). Similarly, Korkmaz *et al.* (2013) attributed the significant dominance of phytane and pristane over *n*-alkane of the Çaglayan Fm. shales of the Sinop Basin to a low maturity. However, many shales and mudstones with low maturity do not have this characteristic (Chen *et al.*, 2001; Korkmaz *et al.*, 2013; Permanyer *et al.*, 2016) and the origin of phytane may play a role in its high abundance. The most common source of phytane is chlorophyll a in phototrophic organisms, and bacteriochlorophyll a and b in purple sulfur bacteria (Brooks *et al.*, 1969; Powell and McKirdy, 1973; Peters *et al.*, 2005b); halophilic bacteria are also assumed to be a nonnegligible source of phytane (Nissenbaum *et al.*, 1972; Anderson *et al.*, 1977). Thus, the presence of lamalginite related to growth of bacteria, has a close connection with this unique phenomenon, and might be the reason for our samples falling out of any given range in the Figure 10. Furthermore, the relatively high abundance of *n*-C_{15} may also indicate bacteria should be a source of the organic matter in our samples. A marked predominance of *n*-C_{17} can be observed in both algae and bacteria, while *n*-C_{15} in green algae is absent or in quite low abundance (Han *et al.*, 1968; Han and Calvin, 1969; Gelpi *et al.*, 1970) and bacteria might be a proper source for the generation of *n*-C_{15}. The presence of hopanoids, related to bacteriohopanepolyols, diploptene or diplopterol (Ourisson *et al.*, 1979; Peters *et al.*, 2005b), indicates that there was also a contribution from bacteria, as these organisms produce all these three kinds of substance.

Regular C_{27}, C_{28}, and C_{29} steranes are generally associated with zooplankton, phytoplankton (diatom), and vascular plants, respectively (Huang and Meinschein, 1979), though some researchers have linked C_{27} regular steranes with marine algae (Adegoke *et al.*, 2014; Gross *et al.*, 2015). If this were the case, algae and vascular plants could be easily distinguished based on the relative abundances of C_{27} and C_{29}. However, Volkman (1986) pointed out that C_{29} regular steranes are not a definitive indicator of a vascular plant source, they can also be derived from green algae, prymnesiophycean algae, and cyanobacteria. In samples O1, O15 and O31, a small component of terrigenous organic matter can be distinguished based on the low abundance of long-chain *n*-alkanes (Peters *et al.*, 2005b). However, the high abundance of C_{29} regular steranes likely reflects

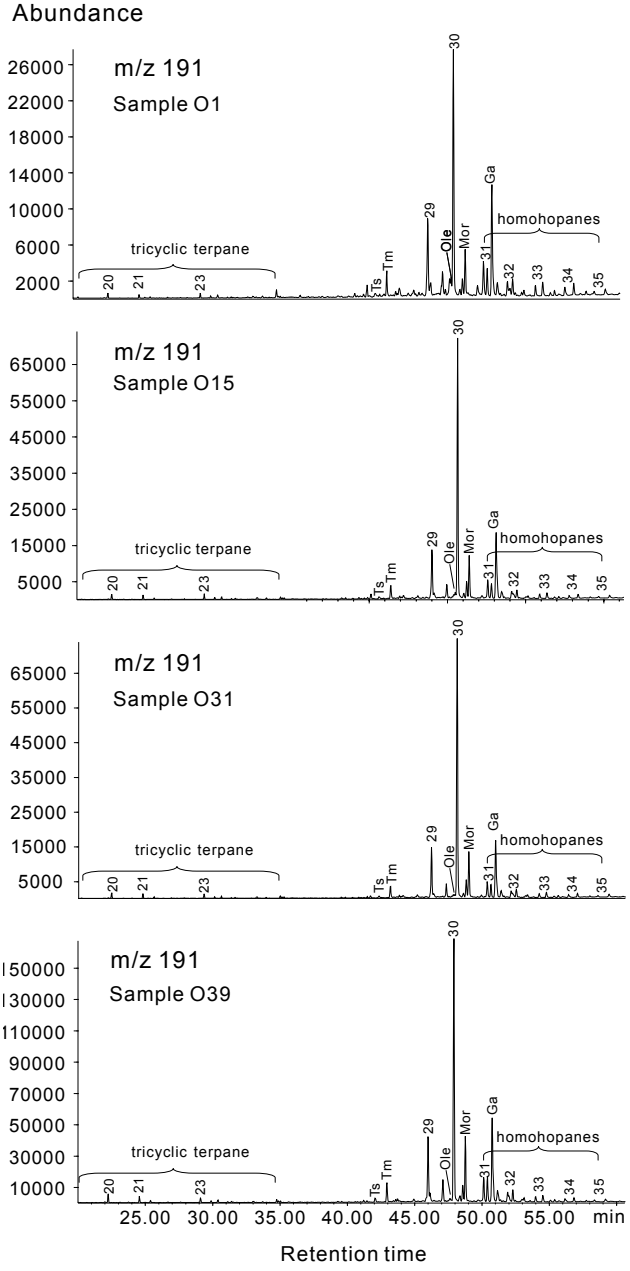

FIGURE 7. Mass chromatograms of the terpanes of laminated mudstones and laminated dolomitic mudstones from the Sha-3-5 submember of the Tanggu area.

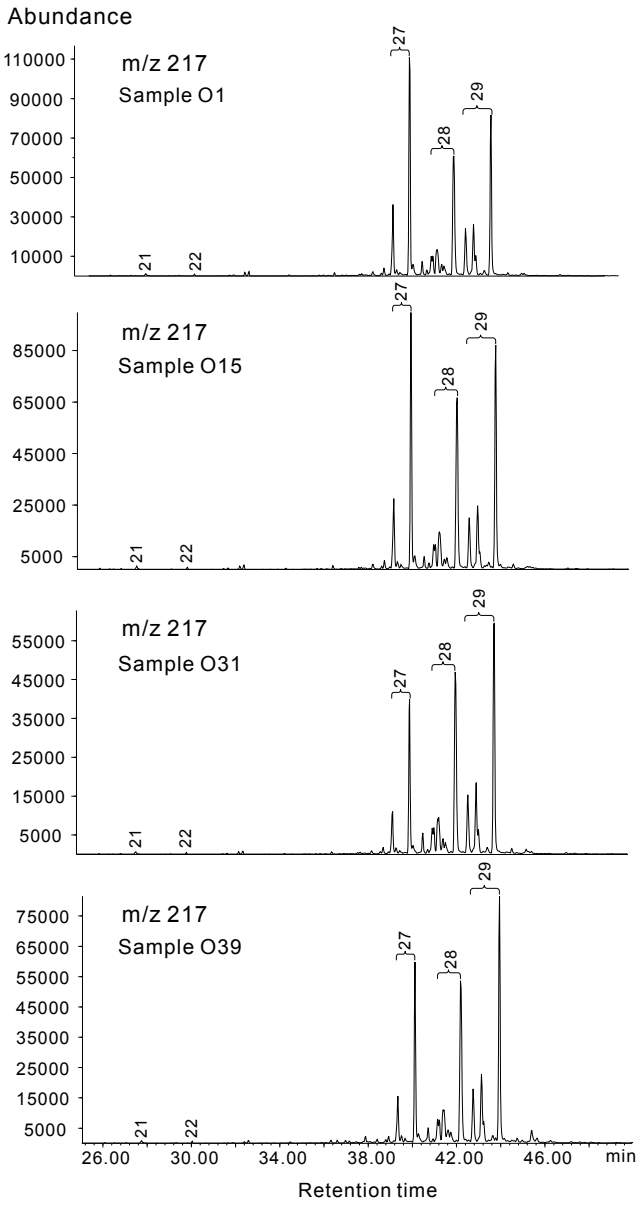

FIGURE 8. Mass chromatograms of the steranes of laminated mudstones and laminated dolomitic mudstones from the Sha-3-5 submember of the Tanggu area. The detailed lithofacies of these samples can be checked in Table 2 by their sample numbers.

an increased contribution from algae or cyanobacteria. Sample O39 shows a complex history (Fig. 8), it has the highest abundance of long-chain *n*-alkanes, the lowest oleanance index, and the highest abundance of C_{29} regular steranes of our sample set. Gelpi *et al.* (1970) documented long-chain (n-C_{27}-n-C_{31}) *n*-alkanes in some species of *Chlorophycophyta*, *Cyanophycophyta*, and *Chrysophycophyta*. Thus, the telalginite we observed is likely to be one of those above-mention species might and can be listed as the major cause for the unique geochemical characteristics in sample O39.

The dinoflagellates *Bohaidina-Parabohaidina* association, an indicator of brackish water, was the predominant type during deposition of the Sha-3 Member in the Huanghua Depression (Zhang, 1991; Yao *et al.*, 1994). However, this association does not occur in the study area; instead, the acritarchs *Dictyotidium*, *Granodisus granulatus* (Mädler, 1963), and *Rugasphacra* predominate (Fig. 5), indicating that the local water chemistry differed from that of the Huanghua Depression. Though acritarchs are generally associated with marine environment (Suárez-Ruiz *et al.*, 2012), the above mentioned three identified species have been reported from both marine successions (Dolby *et al.*, 1979; Lei *et al.*, 2012; Shen *et al.*, 2012) and freshwater deposits (He and Qian, 1979; Yao *et al.*, 1994).

The species identified in our samples is quite different from the species association in the Huanghua Depression, indicating that the succession was deposited in a marine environment. However, this interpretation is not consistent with the lacustrine environment of the Huanghua Depression during deposition of the Sha-3 Member. A lacustrine setting for the Tanggu area is also supported by the relatively low $C_{31}R/C_{30}$ hopane ratio of laminated mudstones and laminated dolomitic mudstones (<0.25, Table 3) (Peters *et al.*, 2005b). A transient ingress of marine water into the Huanghua Depression might be a plausible explanation for the contradiction between the marine interpretation and lacustrine background (Yuan *et al.*, 2005; Ryder *et al.*, 2012), but we lack sufficient evidence to discuss this possibility in detail. Instead, we propose that a saline lacustrine environment fits best the available data.

Organic geochemical characteristics of laminated mudstones and laminated dolomitic mudstones can also indicate the salinity of its depositional environment. Gammacerane is a good indicator of water column stratification induced by hypersalinity in lacustrine environments (Sinninghe Damsté *et al.*, 1995; Peters *et al.*, 2005b). The gammacerane index (10×gammacerane/(gammacerane+C_{30} hopane)) ranges from 2.30 to 3.31 in our samples, suggesting there was a saline lake with high degree of water column stratification.

High salinity is an important factor promoting water column stratification (Boehrer and Schultze, 2008), and persistent stratification is favorable for the development of anoxic bottom water conditions (Demaison and Moore, 1980). The Pr/Ph ratio ranges from 0.22 to 0.37 in our samples, suggesting deposition in an anoxic environment (Didyk *et al.*, 1978). According to ten Haven *et al.* (1987), the inference of anoxia is only justified in hypersaline environments. With the constraint of high salinity, the low Pr/Ph values in our samples are likely to be a reliable indicator of reducing conditions. Despite falling outside any given range, the correlation between Pr/n-C_{17} and Ph/n-C_{18}

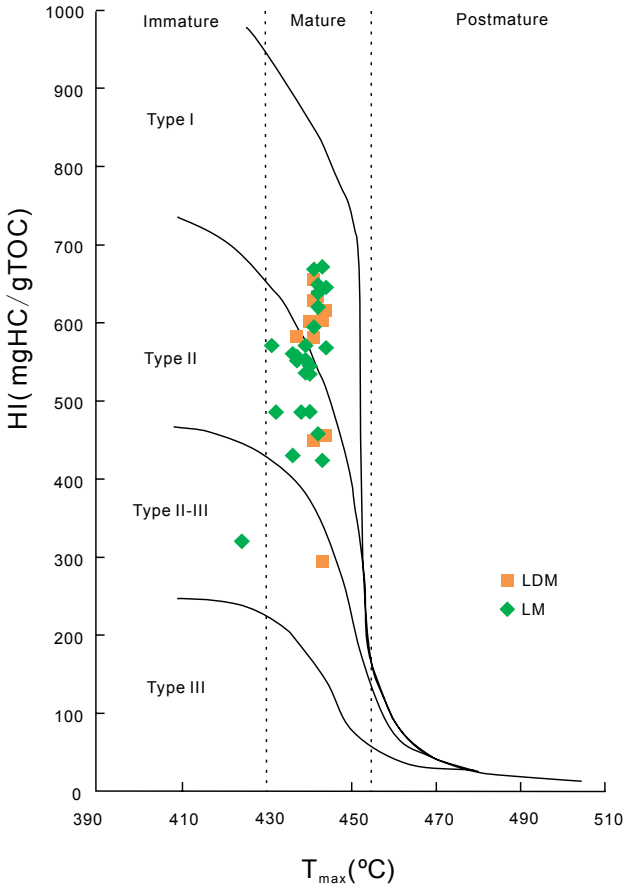

FIGURE 9. Plot of HI *versus* T_{max} of Laminated Mudstones (LM) and Laminated Dolomitic Mudstones (LDM) from the Sha-3-5 submember of the Tanggu area, modified from Mukhopadhyay *et al.* (1995). Kerogen types used to evaluate the ability to yield hydrocarbon are plotted.

suggests that all of our samples were deposited in a strongly reducing environment (Fig. 10). The decreasing trend in the relative abundance of homohopane from C_{31} to C_{35} (Fig. 11) suggests redox conditions during deposition of the source rocks (Peters *et al.*, 2005b). Several sedimentary features such as well-preserved organic matter, intact laminae, and absence of bioturbation may also record reducing conditions.

Potential effects of hydrothermal activity

Two important components of lacustrine mudstones, analcime and dolomite, have been interpreted as diagenetic minerals. Analcime can form via the reaction of precursor materials (clay minerals or plagioclase) with saline-alkaline waters (Gall and Hyde, 1989; Remy and Ferrell, 1989; Renaut, 1993; Do Campo *et al.*, 2007). Dolomite precipitates from Mg-enriched pore brines, or forms via dolomitization of other carbonate precursors (Remy and Ferrell, 1989; Renaut, 1993). Thus, a saline and alkaline environment is a prerequisite for the formation of these two minerals, particularly analcime. However, the hydrothermal sedimentation hypothesis proposes that analcime and ankerite in the rock laminae are syndepositional deposits that precipitated when mantle-derived hydrothermal fluids erupted from migration conduits and spread out over the lake floor (Zheng *et al.*, 2006; Wen *et al.*, 2013); if this were the case, the salinity and alkalinity of the original lake water would have been less important in the formation of the two minerals. Earlier studies focused mainly on the origin of dolostones in the Sha-3-5 submember (Wang *et al.*, 2014), and did not take hydrothermal effects into account. Therefore, it is still unknown whether hydrothermal events occurred, and whether they enhanced the salinity and alkalinity of the ancient lake, however, the saline sedimentary environment of the lake is well substantiated by our organic petrology and geochemistry results.

If the analcime-bearing dolostones correspond to a period of intense hydrothermal fluid eruption, the overlying analcime- and ankerite- bearing mudstones could indicate a period of waning hydrothermal activity. Despite the decreasing flux of hydrothermal fluids, high-temperature thermal alteration of organic matter could potentially be reflected in: i) an increased degree of thermal maturity over a brief geologic interval; ii) the presence of petroleum products related to hydrothermal activity (Simoneit, 2003). If these features can be distinguished in the Sha-3-5 submember, they would constitute compelling evidence for hydrothermal activity.

The Tanggu area did not have high thermal background compared to adjacent areas during deposition of the Sha-3 Member, as seen in the relatively low R_o values (Fig. 12A). One local thermal anomaly does occur, and raises the R_o value drastically in the shallowest (2500-3000m) interval of Well T20 (Fig. 12B), but this is likely due to the magma intrusion rather than hydrothermal activity (Xiao *et al.*, 2004). The R_o

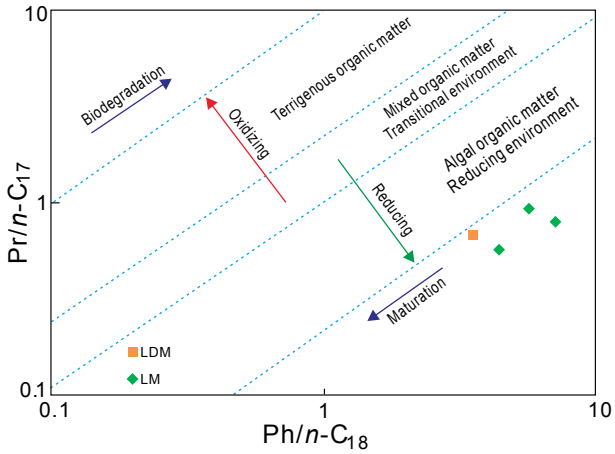

FIGURE 10. Plot of Ph/*n*-C_{18} *versus* Pr/*n*-C_{17} of Laminated Mudstones (LM) and Laminated Dolomitic Mudstones (LDM) from the Sha-3-5 submember of the Tanggu area, modified from Shanmugam (1985).

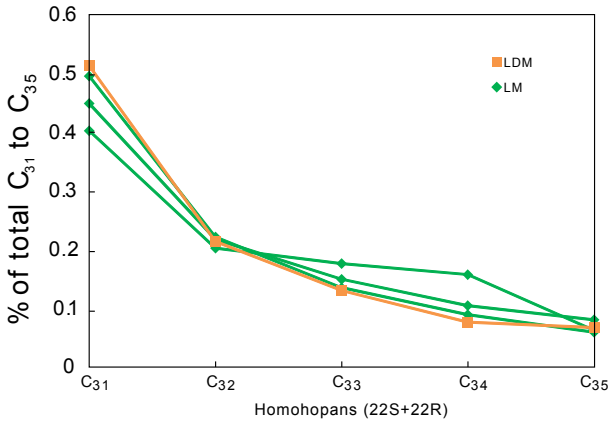

FIGURE 11. Homohopane distributions of laminated mudstones and laminated dolomitic mudstones from the Sha-3-5 submember of the Tanggu area, modified from Peters *et al.* (2015a).

values of other wells also exhibit linear trends with burial depth, and R_o data from Well T20, distal from the intrusive body, follow this trend as well. However, because two measurements from Well T12C deviate slightly from the trend line, R_o data cannot be used to rule out the possibility of thermal alteration via hydrothermal activity. Therefore, other parameters need to be assessed to fully evaluate the thermal maturity.

Stratigraphic variation in T_{max} is minor (Fig. 12), which would require a consistent flux of hydrothermal fluids at a stable temperature. Tissot *et al.* (1987) pointed out that T_{max} thermal maturity assessments are more reliable when type II and type III kerogen predominate over type I. However, the difference in sensitivity is not pronounced when T_{max} values are below 450ºC on the T_{max}-R_o plot (Engel and Macko, 1993), allowing type I kerogen to have a certain reference value. T_{max} does not change concurrently with abrupt increases in abundance of major elements Na, Al, Mg, Ca, and Fe (Fig. 13). Since the elemental composition reflects the presence of analcime and ankerite, the lack of vertical variation in T_{max} suggests that no abnormal thermal events occurred during deposition.

The range of T_{max} values (424–444°C) indicates that organic matter is at the immature to early mature stage, equivalent to R_o values of 0.5 to 0.8 (Waples, 1985; Peters and Cassa, 1994). Other biomarkers and organic petrological parameters indicate a similar level of maturity. The C_{29} ββ/(αα+ββ)) and 20S/(20S+20R) ratios in steranes range from 0.21 to 0.24 and 0.20 to 0.25 respectively, reflecting thermal immaturity (Waples and Machihara, 1991; Peters *et al.*, 2005b). The moretane/hopane ratio ranges from 0.16 to 0.23, indicating that the samples are at the earliest stage of maturity (Waples and Machihara, 1991). T_s/T_m ratio ranges from 0.22 to 0.30, though bearing source and diagenesis information (Moldowan *et al.*, 1986), suggesting low thermal feature herein because of similar kerogen type and its narrow

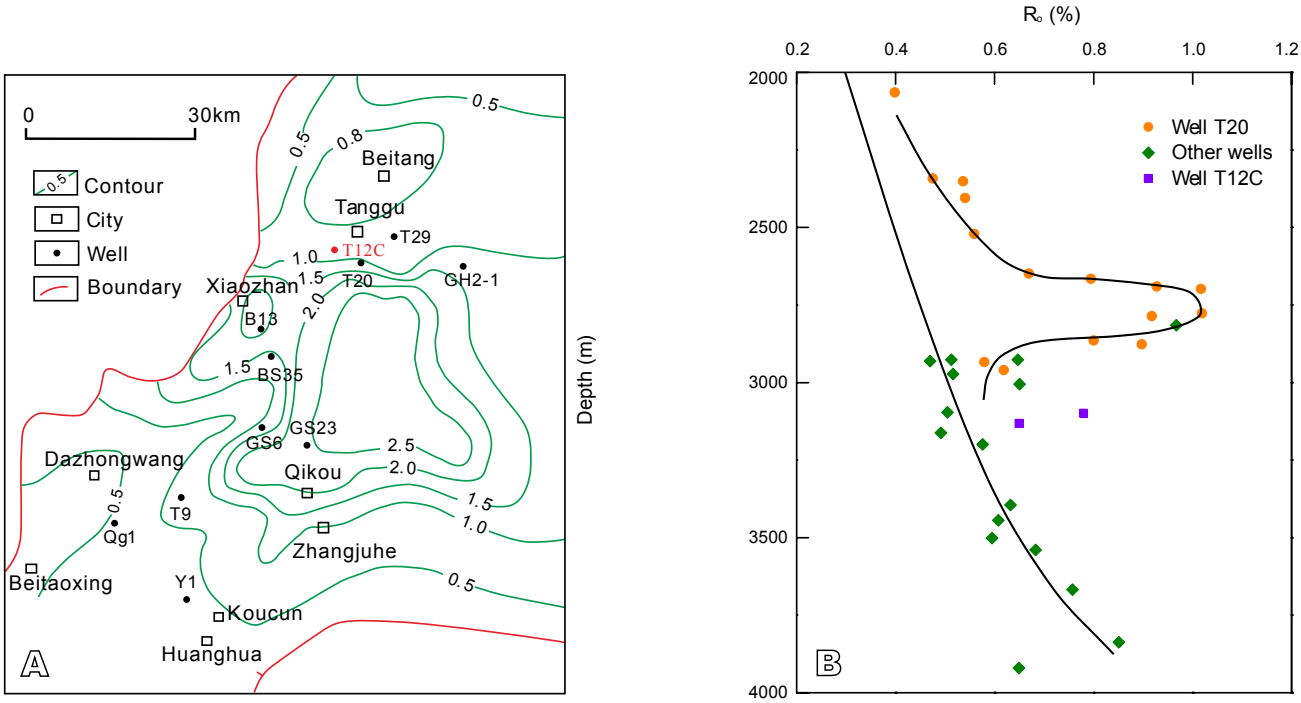

FIGURE 12. Distribution of R_o in the Sha-3 member of the Tanggu area: A) contour maps of R_o value of the Sha-3 member in the central-north of the Huanghua Depression, modified from He *et al.* (2016); B) relationship between R_o and burial depth in the Tanggu area, modified from Xiao *et al.* (2004). The location and R_o data of well T12C were later added in A) and B), respectively.

range. The ratio of C_{31} 22S/(22S+22R) homohopanes ranges from 0.52 to 0.60, seemingly indicating that organic matter is highly mature. This contradicts the previous results, and may be due to sulphurization of hopanoids, which affects isomerization in low-mature organic- and sulfur-rich carbonate-marlstone rocks (Köster *et al.*, 1997). The lowest T_{max} value and highest C_{31} 22S/(22S+22R) ratio occur in sample O1, supporting this conclusion. The Thermal Alteration Index (TAI) and Acritarch Alteration Index (AAI), two color-based maturation indices, are also consistent with the analysis above. The TAI is around 2 to 2.4, based on the pale-yellow to golden-yellow color of preserved pollen (Marshall, 1991; Suárez-Ruiz *et al.*, 2012), and the AAI is roughly 2 to 3 based on the light-yellow to yellow color of the acritarchs (Legall *et al.*, 1981; Marshall, 1991). Both reflect a low level of thermal maturity.

Bai *et al.* (2011) reconstructed the burial and thermal history of the Tanggu area, and suggested that the present-day burial temperature should represent the maximum burial temperature. Considering the bottomhole static temperature of Well T12C (110ºC at 3052.50m) and the geothermal gradient (32.3ºC/km), we can estimate that the present-day burial temperature of the Sha-3-5 submember does not exceed 114ºC. Vitrinite reflectance geothermometry (Barker and Pawlewicz, 1994) and the AAI (Legall *et al.*, 1981) were used to calculate the maximum paleotemperature. Based on the estimated R_o, the calculated maximum paleotemperature is in the range of 80-118ºC by burial heating mechanism. Based on the AAI value, the maximum paleotemperature falls roughly into the 50-90ºC range. In addition, the abundant analcime veins in dolomitic facies of the Sha-3-5 submember (Li *et al.*, 2015a) exhibit characteristics associated with a high-temperature origin (homogenization temperatures: >260ºC, unpublished data). In combination with the small difference between the maximum calculated paleotemperatures and the present-day burial temperature, we conclude that burial heating rather than hydrothermal alteration is likely to be the dominant factor.

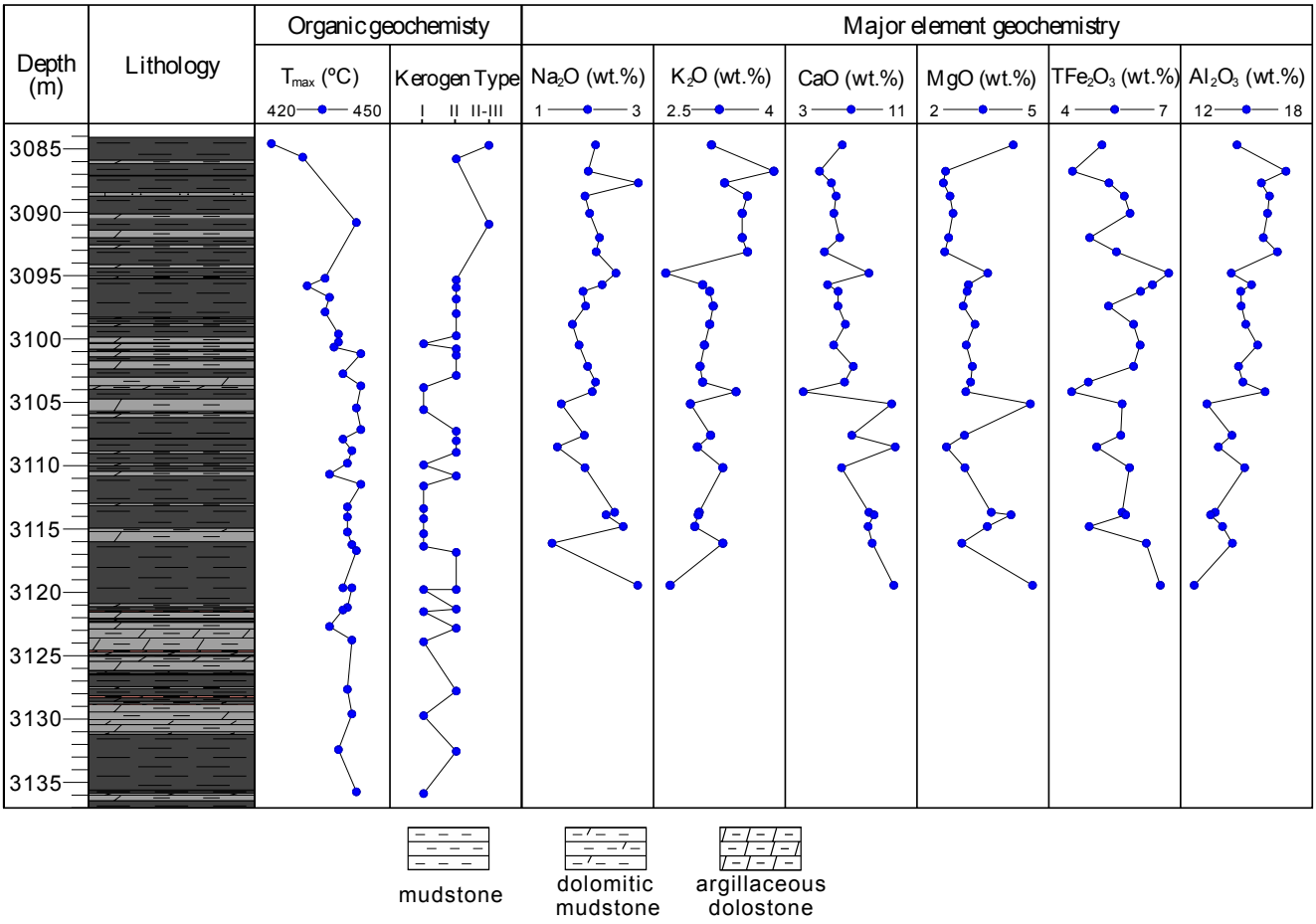

FIGURE 13. Vertical profile of organic geochemistry and major element geochemistry of laminated mudstones and laminated dolomitic mudstones from the Sha-3-5 submember of the Tanggu area. Major element data are from Li *et al.* (2015b).

The calculated paleotemperatures and homogenization temperatures can be compared to two modern analogues, namely, the hydrothermal system associated with the Mid-Atlantic Ridge (~350ºC) (Brault and Simoneit, 1989), and the Waiotapu geothermal region of New Zealand (<100ºC) (Czochanska *et al.*, 1986). As different as many aspects of these hydrothermally altered petroleum systems are, both show a common characteristic: Unresolved Complex Mixtures (UCM) of organic matter superimposed on the *n*-alkane pattern. UCM is a common feature of nearly all hydrothermally-altered sediments (Simoneit, 2003), regardless of the temperature of the hydrothermal fluid. However, the presence of UCM can also result from the weathering of ancient rocks (Peters *et al.*, 2005a) or microbial alteration (Simoneit, 1993). Thus, the absence of UCM does not necessarily indicate the occurrence of hydrothermal alteration.

Based on the above lines of evidence, we propose that hydrothermal activity had a negligible effect on the chemistry of the depositional lake. Instead, the mineral assemblages are compatible with the inferred saline environment and with diagenetic reactions seen in modern and ancient saline-alkaline lakes. In a study of Plio-Pleistocene sediments from Lake Turkana, Kenya, Cerling (1979) proposed that the alteration of montmorillonite to Mg-free zeolite can increase the Mg concentration in interstitial waters, promoting the precipitation of dolomite. Renaut (1993) expanded on this idea, proposing the formula: smectite+Na^{+}+calcite= analcime+dolomite+Ca^{2+}, based on a study of diagenesis in late Quaternary fluviolacustrine sediments from the Lake Bogoria Basin, Kenya. Although Lake Bogoria is fed by alkaline hot springs, the above formula is likely applicable to Sha-3-5 submember.

The Rocky Brook Fm. of the Deer Lake Basin is analogous to the Sha-3-5 submember in several ways, presenting similar lithologic associations and mudstones, this formation was interpreted to have been formed in an alkaline, oxic lake under a relatively arid climate regime (Gall and Hyde, 1989; Hamblin *et al.*, 1997). Van Houten (1962) attributed various analcime- and carbonate-rich lithologies in the Upper Triassic Lockatong Fm. to climatic cycles. Lithological associations in the Sha-3-5 submember may also reflect cyclical, climate-driven sedimentation, with the alternation of predominantly detrital laminae during wetter episodes, and with predominantly chemical laminae during drier episodes. During these cycles, the salinity and redox potential of the depositional lake varied in a regular way. Though the effects of climate and marine ingress require further study, we can infer the presence of an ancient saline lake in the Tanggu area, with minimal hydrothermal influence.

CONCLUSIONS

Organic matter in the laminated mudstones and dolomitic mudstones of the lower Shahejie Fm. was derived mainly from algae and bacteria, with a limited contribution from terrigenous plants, and is thermally immature to early mature. The estimated maximum burial temperature is close to the present-day drill-hole temperature, and no thermal anomaly can be detected. Unresolved complex mixtures on the *n*-alkane pattern are absent, and no evidence of hydrothermal activity could be discerned, suggesting that the water chemistry of the depositional lake was not altered by hydrothermal input. Instead, the lower Shahejie Fm. was deposited in a highly saline lake, and the high salinity possibly resulted in water column stratification and bottom-water anoxia.

ACKNOWLEDGMENTS

This work was financially supported by the Dagang Oilfield Company's 4th Oil Production Plant (grant number: DGYT-2012-JS-566) and the Key Laboratory of Tectonics and Petroleum Resources (KLTPR) open fund (grant number: TPR-2016-07). We are also indebted to Prof. Albert Permanyer and an anonymous referee for their constructive suggestions.

REFERENCES

Adegoke, A.K., Abdullah, W.H., Hakimi, M.H., Sarki Yandoka, B.M., 2014. Geochemical characterisation of Fika Formatiadegokeon in the Chad (Bornu) Basin, northeastern Nigeria: Implications for depositional environment and tectonic setting. Applied Geochemistry, 43, 1-12.

Allen, M.B., Macdonald, D.I.M., Xun, Z., Vincent, S.J., Brouet-Menzies, C., 1997. Early Cenozoic two-phase extension and late Cenozoic thermal subsidence and inversion of the Bohai Basin, northern China. Marine and Petroleum Geology, 14(7), 951-972.

Anderson, R., Kates, M., Baedecker, M.J., Kaplan, I.R., Ackman, R.G., 1977. The stereoisomeric composition of phytanyl chains in lipids of Dead Sea sediments. Geochimica et Cosmochimica Acta, 41(9), 1381-1390.

Bai, Y.F., Wang, H., Wang, Z.S., Liao, Y.T., Lin, Z.L., Huang, C.Y., 2011. Thermal evolution modeling and characteristic of source rock of Paleogene in Beitang Sag. Earth Science - Journal of China University of Geosciences, 36(3), 565-571. [in Chinese with English abstract]

Barker, C.E., Pawlewicz, M.J., 1994. Calculation of Vitrinite Reflectance from Thermal Histories and Peak Temperatures. In: Dow, W.G., (ed.). Vitrinite Reflectance as a Maturity Parameter. Washington, American Chemical Society, 216-229.

Boehrer, B., Schultze, M., 2008. Stratification of lakes. Reviews of Geophysics, 46(2), 1-27.

Brassell, S., Eglinton, G., Maxwell, J., Philp, R., 1978. Natural background of alkanes in the aquatic environment. In: Hutzinger, O., Lelyveld, I.H.V., Zoeteman, B.C.J., (eds.). Aquatic pollutants: Transformation and biological effects. Oxford, Pergamon, 69-86.

Brault, M., Simoneit, B.R.T., 1989. Trace petroliferous organic matter associated with hydrothermal minerals from the Mid-Atlantic Ridge at the trans-Atlantic geotraverse 26°N site. Journal of Geophysical Research: Oceans, 94(C7), 9791-9798.

Bray, E.E., Evans, E.D., 1961. Distribution of *n*-paraffins as a clue to recognition of source beds. Geochimica et Cosmochimica Acta, 22(1), 2-15.

Brooks, J.D., Gould, K., Smith, J.W., 1969. Isoprenoid Hydrocarbons in Coal and Petroleum. Nature, 222(5190), 257-259.

Cerling, T.E., 1979. Paleochemistry of Plio-Pleistocene lake Turkana, Kenya. Palaeogeography, Palaeoclimatology, Palaeoecology, 27, 247-285.

Chen, Z.L., Zhou, G.J., Alexander, R., 1994. A biomarker study of immature crude oils from the Shengli oilfield, People's Republic of China. Chemical Geology, 113(1), 117-132.

Chen, J., Qin, Y., Huff, B.G., Wang, D., Han, D., Huang, D., 2001. Geochemical evidence for mudstone as the possible major oil source rock in the Jurassic Turpan Basin, Northwest China. Organic Geochemistry, 32(9), 1103-1125.

Cheng-Yong, C., 1991. Geological characteristics and distribution patterns of hydrocarbon deposits in the Bohai Bay Basin, East China. Marine and Petroleum Geology, 8(1), 98-106.

Cohen, A.S., 2003. Paleolimnology: The History and Evolution of Lake Systems. New York, Oxford University Press, 525pp.

Czochanska, Z., Sheppard, C.M., Weston, R.J., Woolhouse, A.D., Cook, R.A., 1986. Organic geochemistry of sediments in New Zealand. Part I. A biomarker study of the petroleum seepage at the geothermal region of Waiotapu. Geochimica et Cosmochimica Acta, 50(4), 507-515.

Demaison, G.J., Moore, G.T., 1980. Anoxic environments and oil source bed genesis. Organic Geochemistry, 2(1), 9-31.

Deng, R.J., Xu, B., Qi, J.F., Zhang, L.X., Wang, D.L., Yang, H., Li, J.Y., 2006. Sedimentation characteristics and factors affecting the reservoir in Palaeogene Shasan Member of Beitang sag, Huanghua depression. Acta Petrologica et Mineralogica, 25(3), 230-236. [in Chinese with English abstract]

Didyk, B.M., Simoneit, B.R.T., Brassell, S.C., Eglinton, G., 1978. Organic geochemical indicators of palaeoenvironmental conditions of sedimentation. Nature, 272(5650), 216-222.

Do Campo, M., del Papa, C., Jiménez-Millán, J., Nieto, F., 2007. Clay mineral assemblages and analcime formation in a Palaeogene fluvial-lacustrine sequence (Maíz Gordo Formation Palaeogen) from northwestern Argentina. Sedimentary Geology, 201(1–2), 56-74.

Dolby, G., Ford, J.H., Price, R.J., Thorne, B.V.A., 1979. The micropalaeontology, palynology and stratigraphy of the panarctic et Al Chads Creek B-64 Well, Calgary, Geological Survey of Canada (Calgary), 40pp.

Whelan, J. K., and Thompson-Rizer, C. L., 1993. Chemical Methods for Assessing Kerogen and Protokerogen Types and Maturity. In: Engel, M., Macko, S.A., (eds.). Organic geochemistry: principles and applications. Springer Science & Business Media, 861pp.

Espitalié, J., Deroo, G., Marquis, F., 1985. Rock-Eval Pyrolysis and Its Applications. Revue de l'Institut Français du Pétrol, part one, 40(5), 563-579.

Espitalié, J., Deroo, G., Marquis, F., 1985. Rock-Eval Pyrolysis and Its Applications. Revue de l'Institut Français du Pétrol, part two, 40(6), 755-784.

Espitalié, J., Deroo, G., Marquis, F., 1985. Rock-Eval Pyrolysis and Its Applications. Revue de l'Institut Français du Pétrol, part three, 41(1), 73-89.

Farrimond, P., Taylor, A., Telnæs, N., 1998. Biomarker maturity parameters: the role of generation and thermal degradation. Organic Geochemistry, 29(5-7), 1181-1197.

ECPG-Dagang (Editorial Committee of Petroleum Geology of the Dagang Oil Field), 1991. Petroleum Geology of China Vol. 4: Dagang Oil Field. Beijing, Petroleum Industry Press, 436pp. [in Chinese]

Gall, Q., Hyde, R., 1989. Analcime in lake and lake-margin sediments of the Carboniferous Rocky Brook Formation, Western Newfoundland, Canada. Sedimentology, 36(5), 875-887.

Gelpi, E., Schneider, H., Mann, J., Oró, J., 1970. Hydrocarbons of geochemical significance in microscopic algae. Phytochemistry, 9(3), 603-612.

Gross, D., Sachsenhofer, R.F., Bechtel, A., Pytlak, L., Rupprecht, B., Wegerer, E., 2015. Organic geochemistry of Mississippian shales (Bowland Shale Formation) in central Britain: Implications for depositional environment, source rock and gas shale potential. Marine and Petroleum Geology, 59, 1-21.

Hamblin, A.P., Fowler, M.G., Utting, J., Hawkins, D., Langdon, G.S., 1997. Stratigraphy, palynology and source rock potential of lacustrine deposits of the Lower Carboniferous (Visean) Rocky Brook Formation, Deer Lake Subbasin, Newfoundland. Bulletin of Canadian Petroleum Geology, 45(1), 25-53.

Han, J., Calvin, M., 1969. Hydrocarbon distribution of algae and bacteria, and microbiological activity in sediments. Proceedings of the National Academy of Sciences, 64(2), 436-443.

Han, J., McCarthy, E.D., Van Hoeven, W., Calvin, M., Bradley, W., 1968. Organic geochemical studies, II. A preliminary report on the distribution of aliphatic hydrocarbons in algae, in bacteria, and in a recent lake sediment. Proceedings of the National Academy of Sciences, 59(1), 29-33.

He, C.Q., Qian, Z.S., 1979. Early Tertiary dinoflagellates and acritarchs from the Bose Basin of Guangxi. Acta Palaeontologica Sinica, 18(02), 171-187. [in Chinese with English abstract]

He, J.H., Ding, W.L., Li, R.N., Wang, R.Y., Zhao, W., 2016. Forming condition of the continental shale gas of Shahejie Formation in the central-north Huanghua depression and its resource prospect. Petroleum Geology and Recovery Efficiency, 23(1), 22-30. [in Chinese with English abstract]

He, J.Y., Yu, S.Y., 1982. Occurrence of glauconite in Lower Tertiary of northern Huanghua Depression. Earth Science (1), 129-143. [in Chinese with English abstract]

Horsfield, B., Curry, D.J., Bohacs, K., Littke, R., Rullkötter, J., Schenk, H.J., Radke, M., Schaefer, R.G., Carroll, A.R., Isaksen, G., Witte, E.G., 1994. Organic geochemistry of freshwater and alkaline lacustrine sediments in the Green River Formation of the Washakie Basin, Wyoming, U.S.A. Organic Geochemistry, 22(3), 415-440.

Huang, W.-Y., Meinschein, W.G., 1979. Sterols as ecological indicators. Geochimica et Cosmochimica Acta, 43(5), 739-745.

Huang, C.Y., Wang, H., Gao, J.R., Wang, J.H., Liu, J., Yue, Y., Liao, Y.T., 2008. Tectonic evolution and its controlling over sequence filling pattern of Paleogene in Beitang sag. Journal of China University of Petroleum, Edition of Natural Science, 32(3), 7-13. [in Chinese with English abstract]

Huang, C.Y., Wang, H., Zhou, L.H., Ren, P.G., Liu, J., Bai, Y.F., 2009. Provenance system characters of the third Member of Shahejie Formation in the Paleogene in Beitang Sag. Earth Science - Journal of China University of Geosciences, 34(6), 975-984. [in Chinese with English abstract]

Ingles, M., Salvany, J.M., Muñoz, A., Perez, A., 1998. Relationship of mineralogy to depositional environments in the non-marine Tertiary mudstones of the southwestern Ebro Basin (Spain). Sedimentary Geology, 116(3-4), 159-176.

Jian, C., Dewen, L., Yuwen, L., Yong, T., Abulimit, Qiusheng, C., Tingting, W., 2015. Ancient high quality alkaline lacustrine source rocks discovered in the Lower Permian Fengcheng Fromation, Junggar Basin. Acta Petrolei Sinica, 36(7), 781-790. [in Chinese with English abstract]

Korkmaz, S., Kara-Gülbay, R., İztan, Y.H., 2013. Organic geochemistry of the Lower Cretaceous black shales and oil seep in the Sinop Basin, Northern Turkey: An oil-source rock correlation study. Marine and Petroleum Geology, 43, 272-283.

Köster, J., Van Kaam-Peters, H.M.E., Koopmans, M.P., De Leeuw, J.W., Sinninghe Damsté, J.S., 1997. Sulphurisation of homohopanoids: Effects on carbon number distribution, speciation, and 22S22R epimer ratios. Geochimica et Cosmochimica Acta, 61(12), 2431-2452.

Largeau, C., Derenne, S., Casadevall, E., Berkaloff, C., Corolleur, M., Lugardon, B., Raynaud, J.F., Connan, J., 1990. Occurrence and origin of "ultralaminar" structures in "amorphous" kerogens of various source rocks and oil shales. Organic Geochemistry, 16(4), 889-895.

Legall, F.D., Barnes, C.R., MacQueen, R.W., 1981. Thermal maturation, burial history and hotspot development, Paleozoic strata of southern Ontario-Quebec, from conodont acritarch colour alteration studies. Bulletin of Canadian Petroleum Geology, 29(4), 492-539.

Lei, Y., Servais, T., Feng, Q., He, W., 2012. The spatial (nearshore–offshore) distribution of latest Permian phytoplankton from the Yangtze Block, South China. Palaeogeography, Palaeoclimatology, Palaeoecology, 363-364, 151-162.

Li, L., Yao, G.Q., 2016. Primary dolostone related to the Cretaceous lacustrine hydrothermal sedimentation in Qingxi sag, Jiuquan Basin on the northern Tibetan Plateau: Discussion. Science China Earth Sciences, 59(4), 866-870.

Li, L., Yao, G.Q., Liu, Y.H., Hou, X.C., Gao, Y.J., Zhao, Y., Wang, G., 2015a. Characterization of analcime-dolomite reservoir from Shahejie Formation in Tang 10 Block of Dagang Oilfield. Acta Petrolei Sinica, 36(10), 1210-1220. [in Chinese with English abstract]

Li, L., Yao, G.Q., Liu, Y.H., Hou, X.C., Wang, G., Zhao, Y., Gao, Y.J., 2015b. Major and trace elements geochemistry and geological implications of dolomite-bearing mudstones in lower part of Shahejie Formation in Tanggu area, eastern China. Earth Science-Journal of China University of Geosciences, 40(9), 1480-1496. [in Chinese with English abstract]

Liu, Y.Q., Jiao, X., Li, H., Yuan, M.S., Yang, W., Zhou, X.H., Liang, H., Zhou, D.W., Zheng, C.Y., Sun, Q., Wang, S., 2012. Primary dolostone formation related to mantle-originated exhalative hydrothermal activities, Permian Yuejingou section, Santanghu area, Xinjiang, NW China. Science China Earth Sciences, 55(2), 183-192.

Mädler, K.A., 1963, Organic microstructures of the Posidonia Shale. Beihefte zum Geologischen Jahrbuch, 58, 287- 406.

Marshall, J.E.A., 1991. Determination of Thermal Maturity. In: Briggs, D.E.G., Crowther, P., (eds.). Palaeobiology - a synthesis. Oxford, Blackwell Scientific Publications, 511-515.

Moldowan, J.M., Sundararaman, P., Schoell, M., 1986. Sensitivity of biomarker properties to depositional environment and/or source input in the Lower Toarcian of SW-Germany. Organic Geochemistry, 10(4), 915-926.

Morgan, L.A., 2007. Integrated Geoscience Studies in the Greater Yellowstone Area - Volcanic, Tectonic, and Hydrothermal Processes in the Yellowstone Geoecosystem. U.S. Geological Survey, Professional Paper 1717, 532pp.

Mukhopadhyay, P.K., Wade, J.A., Kruge, M.A., 1995. Organic facies and maturation of Jurassic/Cretaceous rocks, and possible oil-source rock correlation based on pyrolysis of asphaltenes, Scotian Basin, Canada. Organic Geochemistry, 22(1), 85-104.

Nissenbaum, A., Baedecker, M.J., Kaplan, I.R., 1972. Organic geochemistry of Dead Sea sediments. Geochimica et Cosmochimica Acta, 36(7), 709-727.

Ourisson, G., Albrecht, P., Rohmer, M., 1979. The Hopanoids: palaeochemistry and biochemistry of a group of natural products. Pure and Applied Chemistry, 51(4), 709-729.

Pacton, M., Gorin, G.E., Vasconcelos, C., 2011. Amorphous organic matter - Experimental data on formation and the role of microbes. Review of Palaeobotany and Palynology, 166(3), 253-267.

Permanyer, A., Baranger, R., Lugardon, B., 1994. Oil shale characterization in Messinian pre-evaporitic sediments from the Lorca basin (South-East Spain). Bulletin du Centre de Recherches de l'Exploration - Production Elf - Aquitaine, 18, 135-149.

Permanyer, A., Jorge, R., Baudino, R., Gibert, L., 2016. Organic-rich shales from internal Betic basins (SE Spain): potential source rocks analogs for the pre-Messinian Salt play in the western Mediterranean. Geologica Acta, 14(4), 443-460.

Peters, K.E., Cassa, M.R., 1994. Applied Source Rock Geochemistry. In: Magoon, L.B., Dow, W.G., (eds.). The Petroleum System – From Source to Trap. Tulsa, American Association of Petroleum Geologists, Memoir 60, 93-117.

Peters, K.E., Walters, C.C., Moldowan, J.M., 2005a. The Biomarker Guide Volume 1: Biomarkers and Isotopes in the Environment and Human History. New York, Cambridge University Press, 471pp.

Peters, K.E., Walters, C.C., Moldowan, J.M., 2005b. The Biomarker Guide Volume 2: Biomarkers and Isotopes in Petroleum Systems and Earth History. New York, Cambridge University Press, 680pp.

Powell, T., McKirdy, D., 1973. Relationship between ratio of pristane to phytane, crude oil composition and geological environment in Australia. Nature, 243(124), 37-39.

Qu, C.W., Lin, C.M., Cai, M.J., Cheng, Y.Z., Wang, B.J., Zhang, X., 2014. Characteristics of dolostone reservoir in Sha3 group from Palaeogene Shahejie Formation in Beitang sag, Bohaiwan Basin. Acta Geologica Sinica, 88(8), 1588-1602. [in Chinese with English abstract]

Remy, R.R., Ferrell, R.E., 1989. Distribution and origin of analcime in marginal lacustrine mudstones of the Green River Formation, South-Central Uinta Basin, Utah. Clays and Clay Minerals, 37(5), 419-432.

Renaut, R.W., 1993. Zeolitic diagenesis of late Quaternary fluviolacustrine sediments and associated calcrete formation in the Lake Bogoria Basin, Kenya Rift Valley. Sedimentology, 40(2), 271-301.

Ryder, R.T., Qiang, J., McCabe, P.J., Nuccio, V.F., Persits, F., 2012. Shahejie-Shahejie/Guantao/Wumishan and Carboniferous/Permian Coal-Paleozoic Total Petroleum Systems in the Bohaiwan Basin, China (based on geologic studies for the 2000 World Energy Assessment Project of the U.S. Geological Survey). Reston, VA, U.S. Geological Survey, Scientific Investigations Report 2011-5011, 89pp.

Schieber, J., Bose, P.K., Eriksson, P., Banerjee, S., Sarkar, S., Altermann, W., Catuneanu, O., 2007. Atlas of microbial mat features preserved within the siliciclastic rock record. Amsterdam, Elsevier, 311pp.

Shanmugam, G., 1985. Significance of coniferous rain forests and related organic matter in generating commercial quantities of oil, Gippsland Basin, Australia. American Association of Petroleum Geologists (AAPG) Bulletin, 69(8), 1241-1254.

Shen, J., Algeo, T.J., Zhou, L., Feng, Q., Yu, J., Ellwood, B., 2012. Volcanic perturbations of the marine environment in South China preceding the latest Permian mass extinction and their biotic effects. Geobiology, 10(1), 82-103.

Simoneit, B.R.T., 1993. Hydrothermal Alteration of Organic Matter in Marine and Terrestrial Systems. In: Engel, M.H., Macko, S.A., (eds.). Organic Geochemistry: Principles and Applications, Boston, MA, U.S.A, Springer, 397-418.

Simoneit, B.R., 2003. Petroleum generation, extraction and migration and abiogenic synthesis in hydrothermal systems. In: Ikan, R., (ed.). Natural and Laboratory-Simulated Thermal Geochemical Processes. Netherlands, Springer, 1-30.

Sinninghe Damsté, J.S., Kenig, F., Koopmans, M.P., Köster, J., Schouten, S., Hayes, J.M., de Leeuw, J.W., 1995. Evidence for gammacerane as an indicator of water column stratification. Geochimica et Cosmochimica Acta, 59(9), 1895-1900.

Song, B.R., Han, H.D., Cui, X.D., Dong, X.D., Chen, J.M., 2015. Petrogenesis analysis of lacustrine analcite dolostone of the Member 4 of Paleogene Shahejie Formation in Liaohe Depression, Bohai Bay Basin. Journal of Palaeogeography, 17(1), 33-44. [in Chinese with English abstract]

Suárez-Ruiz, I., Flores, D., Mendonça Filho, J.G., Hackley, P.C., 2012. Review and update of the applications of organic petrology: Part 1, geological applications. International Journal of Coal Geology, 99, 54-112.

Sun, Z.C., Peng, L.C., Li, D.M., Wang, M., 1996. Relationship between eustasy and transgression in early Tertiary in eastern China. Geological Review, 42(S1), 181-187. [in Chinese with English abstract]

ten Haven, H.L., de Leeuw, J.W., Rullkotter, J., Damste, J.S.S., 1987. Restricted utility of the pristane/phytane ratio as a palaeoenvironmental indicator. Nature, 330(6149), 641-643.

Tiercelin, J.-J., Pflumio, C., Castrec, M., Boulégue, J., Gente, P., Rolet, J., Coussement, C., Stetter, K.O., Huber, R., Buku, S., Mifundu, W., 1993. Hydrothermal vents in Lake Tanganyika, East African, Rift system. Geology, 21(6), 499-502.

Tissot, B.P., Pelet, R., Ungerer, P., 1987. Thermal history of sedimentary basins, maturation indices, and kinetics of oil and gas generation. American Association of Petroleum Geologists (AAPG) Bulletin, 71(12), 1445-1466.

Tu, J.Q., Chen, J.P., Zhang, D.J., Cheng, K.M., Chen, J.J., Yang, Z.M., 2012. A petrographic classification of macerals in lacustrine carbonate source rocks and their organic petrological characteristics: A case study on Jiuxi basin, NW China. Acta Petrologica Sinica, 28(3), 917-926. [in Chinese with English abstract]

Tyson, R.V., 1995. Sedimentary organic matter: organic facies and palynofacies. Chapman & Hall, London, 169-180, 344.

Van Houten, F.B., 1962. Cyclic sedimentation and the origin of analcime-rich Upper Triassic Lockatong Formation, west-central New Jersey and adjacent Pennsylvania. American Journal of Science, 260(8), 561-576.

Volkman, J.K., 1986. A review of sterol markers for marine and terrigenous organic matter. Organic Geochemistry, 9(2), 83-99.

Wang, B.J., Cai, M.J., Lin, C.M., Zhang, X., Cheng, Y.Z., Qu, C.W., Zhang, N., 2014. Characteristics and origin of lacustrine dolostone of the Paleogene Shahejie Formation in Tanggu area, Bohai Bay Basin. Journal of Palaeogeography, 16(1), 65-76. [in Chinese with english abstract]

Waples, D.W., 1985. Geochemistry in petroleum exploration. Netherlands, Springer, 403pp.

Waples, D.W., Machihara, T., 1991. Biomarkers for geologists-A practical guide to the application of steranes and triterpanes in petroleum geology. Tulsa, American Association of Petroleum Geologists (AAPG) Methods in Exploration, No. 9, 91pp.

Wen, H.G., Zheng, R.C., Qing, H.R., Fan, M.T., An, L.Y., Shi, G.B., 2013. Primary dolostone related to the Cretaceous lacustrine hydrothermal sedimentation in Qingxi sag, Jiuquan Basin on the northern Tibetan Plateau. Science China: Earth Sciences, 56(12), 2080-2093. [in Chinese]

Xiao, K.Y., Deng, R.Y., Yang, H., Xiao, D.Q., Wei, A.J., Xu, B., Li, J.Y., Gao, H., 2004. Petroleum geological role of magmatic activities in Xingang prospect area, Beitang sag. Petroleum Exploration and Development, 31(2), 25-28. [in Chinese with English abstract]

Yang, R., Cao, J., Hu, G., Fu, X., 2015. Organic geochemistry and petrology of Lower Cretaceous black shales in the Qiangtang Basin, Tibet: Implications for hydrocarbon potential. Organic Geochemistry, 86, 55-70.

Yao, Y.M., Xu, J.L., Shan, H.G., Li, J.R., 1992. A discussion of the Paleogene transgression in the Jiyang Depression, Shandong Province. Acta Petrolei Sinica, 13(2), 29-34. [in Chinese with English abstract]

Yao, Y.M., Liang, H.D., Cai, Z.G., Guan, X.T., Zhao, Z., Chen, Z., Sun, Z., Yang, S., 1994. Tertiary in Petroliferous Regions of China (IV): The Bohaiwan Basin, Beijing. Petroleum Industry Press, 26-76; 102-144. [in Chinese]

Yuan, W.F., Chen, S.Y., Zeng, C.M., 2005. Research development and prospects on Paleogene sea transgression in Bohai Bay Basin. Acta Sedimentologica Sinica, 23(4), 604-612. [in Chinese with English abstract]

Yuan, W.F., Chen, S.Y., Zeng, C.M., 2006. Study on marine transgression of Paleogene Shahejie Formation in Jiyang Depression. Acta Petrolei Sinica, 27(4), 40-44+49. [in Chinese with English abstract]

Zhang, F.M., 1991. Stratigraphy and the Tertiary sedimentary environment. In: Editorial Committee of Petroleum Geology of the Dagang Oil Field (ed.), Vol. 4: Petroleum geology of China. Beijing, Petroleum Industry Press, 32-73.

Zhang, T.T., Wang, H., Yue, Y., Huang, C.Y., Zhang, L.W., 2009. Cenozoic subsidence features of Beitang sag and relationship with tectonic evolution. Journal of Earth Science, 20(4), 746-754.

Zheng, R.C., Wen, H.G., Fan, M.T., Wang, M.F., Wu, G.X., Xia, P.F., 2006. Lithological characteristics of sublacustrine white smoke type exhalative rock of the Xiagou Formation in Jiuxi Basin. Acta Petrologica Sinica, 22(12), 3027-3038. [in Chinese with English abstract]

Zhou, L.H., Lu, Y., Xiao, D.Q., Zhang, Z.P., Chen, X.B., Wang, H., Hu, S.Y., 2011. Basinal texture structure of Qikou Sag in Bohai Bay Basin and its Evolution. Nature Gas GeoScience, 22(3), 373-382. [in Chinese with English abstract]

Zhong, D.K., Jiang, Z.C., Guo, Q., Sun, H.T., Yang, Z., 2015. Discovery of hydrothermal dolostones in Baiyinchagan sag of Erlian Basin, Inner Mongolia, and its geologic and mineral significance. Oil & Gas Geology, 36(4), 587-595. [in Chinese with English abstract]

Manuscript received April 2017;
revision accepted September 2017;
published Online January 2018.